Analysis of the molecular mechanisms maintaining the higher order structure of the Golgi apparatus

2015

Jeerawat Soonthornsit

Division of Engineering

Graduate School of Kyoto Sangyo University

Table of Contents

Abbreviation **1**

Abstract **2**

General introduction **4**

***Chapter I*. The disassembly of Golgi apparatus and its mediated factors under acidic extracellular pH condition** **8**

Introduction **9**

Results **11**

The reversible disassembly of Golgi apparatus induced by low pH medium 11

All Golgi compartments were disassembled and *cis*-Golgi was disassembled prior to the other compartment. 12

Anterograde transport was delayed under the low pH condition. 12

No effect in actin structure under low pH treatment. 13

PLA_2 inhibitors protected Golgi disassembly induced by low pH treatment. 14

The Rab1 suppressed the Golgi disassembly and dispersal under low pH treatment 15

The overexpression of Rab1 did not rescue anterograde transport under low pH treatment 15

High temperature negated the Rab1 function for suppressing the Golgi disassembly 16

Discussions **18**

***Chapter II*. The localization of YIPF1, YIPF2 and YIPF6 and their functions** **23**

Introduction **24**

Results **26**

YIPF1, YIPF2 and YIPF6 localized in *medial*-, *trans*-Golgi and TGN 26

Knockdown of YIPF1, YIPF2 and YIPF6 27

YIPF1, YIPF2 and YIPF6 knockdown reduced the disassembly of *medial*-, *trans*-Golgi and TGN induced by the low pH treatment 27

YIPF1 and YIPF2 knockdown reduced the glycoprotein production 29

Discussions **30**

Materials and Methods **32**

Cell culture and pH conditioned media **32**

Drug treatment **32**

Transfection and RNA interference **33**

SDS-Page and Western blot analysis **34**

Immunofluorescence staining **35**

Anterograde protein transport assay **36**

Electron microscopy 36
Periodic acid-Schiff (PAS) staining 37
Quantitative analysis of the Golgi structure 38

Acknowledgements 39

References 40

Figure Legends 48
Figure 1 53
Figure 2 54
Figure 3 55
Figure 4 56
Figure 5 57
Figure 6 58
Figure 7 60
Figure 8 61
Figure 9 62
Figure 10 63
Figure 11 64
Figure 12 65
Figure 13 66
Figure 14 67
Figure 15 69
Figure 15 70
Figure 16 71

Abbreviation

AACOCF3: Arachidonyl trifluoromethyl ketone

ARF: ADP-ribosylation factors

BEL: Bromoenol lactone

COG: Conserved oligomeric

COPI: Coat protein I

COPII: Coat protein II

cPLA2α: Ca^{2+}-dependent PLA_2-α

ER: Endoplasmic reticulum

GalT: β1,4-galactosyl transferase

GAP: GTPase-activating proteins

GFP: Green fluorescent protein

GlcNAcT1: β-1,3-N-acetylglucosaminyl transferase I

HA: Human influenza hemagglutinin

iPLA2-β: Ca^{2+}-independent PLA_2-β

LIS1: lissencephaly1

MAFP Methyl arachidonyl fluorophosphonate

ONO: ONO-RS-082

PAFAH Ib: Platelet-activating factor acetylhydrolase

PAS: periodic acid-schiff reaction

PLA_2: Phospholipase A_2

RFP: Red fluorescent protein

SD: Standard deviation

SNARE: soluble N-ethylmaleimide-sensitive factor attachment protein receptor

TGN: *Trans*-Golgi network

VSV-G: Vesicular stomatitis virus glycoprotein

wt: Wild type

Yip1p: Ypt-interacting protein

Abstract

The Golgi apparatus is a membranous organelle that plays an essential role in proteins and lipids transport between intracellular organelles along the secretory pathway. The Golgi apparatus has a stacked cisternal and polarized structure, which is thought to have important role for the post-translational modifications, sorting and the transport of cargo proteins. Golgi apparatus has a highly dynamics structure which is maintained by a balance of incoming and outgoing tubular and vesicular carriers. These carriers are involved in the transport of variety cargoes, which pass through the Golgi cisternae. In mammalian cells, Golgi stack are connected to form a ribbon-like higher order structure near the centriole. This structure is proposed to have importance for polarized transport of proteins. However, the molecular mechanisms to maintain the ribbon like structure are not well understood. I took two approaches to understand the molecular mechanisms underlying the formation of the Golgi ribbon. First is the analysis of the Golgi disassembly induced under low pH treatment. Second is the analysis of function of the multi-span membrane proteins localized in the Golgi apparatus.

In ***chapter I***, I described the results obtained from the first approach. Low pH medium induced the disassembly of the whole of the Golgi apparatus, *cis*-Golgi, *medial*-/ *trans*-Golgi and TGN (*trans*-Golgi network) with all the compartments remained separated. *Cis*-Golgi markers were observed in tubular structures in early stage after changing to the low pH medium, while *medial*-/ *trans*-Golgi and TGN were not observed in tubular structures. The ribbon like-structure of the Golgi apparatus was completely recovered after returning to the control pH medium. Low pH medium did not only change the Golgi structure but also perturbed the function. The anterograde transport of VSV-G tsO45-GFP protein was significantly inhibited. The Golgi disassembly was clearly inhibited by ONO-RS-082 (ONO) and Bromoenol lactone (BEL), Phospholipase A_2 (PLA_2) antagonists, which were expected to

inhibit the tubule formation from the Golgi membrane, and also by the expression of Rab1, which was though to increase the vesicle fusion. These results suggested that the disassembly of the Golgi apparatus induced by low pH medium was regulated by PLA_2 and Rab1.

In ***Chapter II***, I described the results for the second approach. It has been shown that a family of five span transmembrane proteins, named YIPF, are localized in the Golgi apparatus and involved in the maintenance of the ribbon-like Golgi structure. The localization and function of YIPF1, YIPF2 and YIPF6 were investigated. These proteins mainly localized in *medial-*, *trans*-Golgi and TGN and relocated together with these three compartment markers after the Golgi disassembly in a low pH medium. The knockdown of YIPF6 reduced to the stability of YIPF1 and YIPF2. Surprisingly, the reduction of YIPF1, YIPF2 or/and YIPF6 significantly suppressed the disassembly of *medial-*, *trans*-Golgi and TGN in the low pH condition. On the other hand, YIPF1 or/and YIPF2 knockdown reduced the synthesis of glycoproteins. These results suggested that YIPF1, YIPF2 and YIPF6 involved in the disassembly of *medial-*, *trans*-Golgi and TGN under low pH condition, and the balance of them was important for the glycoprotein synthesis in the Golgi apparatus.

Taken together I propose that low pH treatment is a new analytic tool for analyzing the mechanism maintaining the higher order structure of the Golgi apparatus. Furthermore, I suggest that PLA_2, YIPF1, YIPF2 and YIPF6 promote the disassembly of the Golgi apparatus under low pH and Rab1 counteracts this process.

General introduction

The Golgi apparatus is a membranous organelle and plays an essential role in proteins and lipids processing, modification and sorting. Newly synthesized proteins and lipids from the endoplasmic reticulum (ER) are transported to Golgi membrane, and then post-translational modifications, including glycosylation, are performed (Shorter and Warren, 2002). After passing through the Golgi apparatus, the product proteins and lipids are sorted and sent to their final destinations, such as plasma membrane and lysosomes (Keller and Simon, 1997). The stack is polarized into *cis*-, *medial*-, *trans*-Golgi cisternae and *trans*-Golgi network (TGN) and Golgi resident enzymes are localized according to the order of their functions (Rambourg and Clermont, 1990). Proteins enter the Golgi at *cis*-Golgi compartment and pass thru *medial*- and *trans*-Golgi compartments. The biosynthesis of cargo proteins undergoes the modifications, including glycosylation (Stanley, 2011). Then they are sorted and exited at TGN to downstream destinations (Keller and Simon, 1997).

The newly synthesized proteins are transported out from the ER by COPII vesicles toward the Golgi apparatus. The arriving COPII vesicles from ER are tethered and fused on the *cis*-side (*cis*-Golgi network, CGN/ ER-Golgi intermediate compartment, ERGIC) of the Golgi apparatus (Appenzeller-Herzog and Hauri, 2006). Secretory proteins are conveyed through *cis*-, *medial*- and *trans*-Golgi compartments with adding and/or removing glycan residues by several glycosylation enzymes (Brockhausen 1999; Schwarz and Aebi, 2011). Finally, cargo proteins are sorted by specific transport carriers, including clathrin-coated and non-clathrin-coated vesicles, at *trans*-Golgi network (TGN) and transported out to their final destinations (Kienzle and von Blume, 2014). Some Golgi residential enzymes and membrane proteins are recycled from the Golgi apparatus to the ER by COPI vesicles (Orci *et al.*, 2000; Beck *et al*., 2009).

At least two models for intra-Golgi transport are proposed. In vesicular transport model, a stack is a stable component and secretory proteins are transported across the stack by transport vesicles that bud from one cisterna and fuse with the next in anterograde transport vesicles. In the cisternal progression/maturation model, ER-derived carriers are fused and form a new *cis*-cisterna at the *cis*-side of the stack. The cisterna gradually matures into a *medial*, a *trans* and then a TGN cisterna while resident Golgi proteins are recycled back to upstream cisternae by COPI vesicles (Glick and Luini, 2011).

In higher eukaryotic cells, especially in vertebrate cells, the Golgi apparatus is assembled to form a ribbon-like structure at a perinuclear area near the centriole. The ribbon-like structure of the vertebrate Golgi apparatus is proposed to have important roles for the cell polarization (Bisel *et al*., 2008). However, the mechanism for the maintenance of the Golgi structure, especially the formation of the ribbon-like structure, remains obscure. To understand this, artificial disruption of the Golgi structure has been employed in many instances. The structure of the Golgi apparatus is disturbed by various treatments such as temperature change, cellular stress and chemical compounds that affect the secretory pathway. For example, at 20°C, the transport out of the Golgi is blocked and a large bulging domains in *trans*-side cisternae (Ladinsky *et al*., 2002). During apoptosis, the Golgi complex is dramatically disassembled due to changes in the Golgi structural proteins (Hick and Machamer, 2005). The disassembly of Golgi apparatus was also found in hyper-excitable neurons from increased potassium concentration (Thayer *et al.*, 2013). During cell cycle, the Golgi apparatus disassembles when a cell enters into mitosis and reassembles after the cell division. Mitotic fragmentation of the Golgi is triggered by CDK1/cyclin B that inhibits transport vesicle fusion to the Golgi cisternae, while the vesicle budding from the Golgi cisternae remains constant (Warren *et al*., 1995; Nakamura *et al*., 1997; Lowe *et al*., 1998). A fungal metabolite Brefeldin A (BFA), blocks ER-to-Golgi and intra-Golgi vesicular transport

of secretory and membrane proteins. BFA treatment causes recycling back of Golgi resident enzymes to ER leading to the Golgi disassembly (Lippincott-Schwartz *et al*., 1989; Wagner *et al*., 1994; Niu *et al*., 2005). In my laboratory, it was found that Golgi apparatus quickly disassembles in a low pH medium. However, the mechanism of the Golgi disassembly was not investigated. Therefore, I decided to clarify the mechanism of the low pH induced Golgi disassembly to obtain a clue to understand the mechanism of the maintenance of the Golgi structure. The results of this analysis was described and discussed in ***Chapter I.***

The structure of the Golgi apparatus is highly dynamic and has to be maintained by the balance of input and output of vesicular and tubular carriers (Mollenhauer and Morré, 1993; Ward *et al*, 2001). Excess vesicle budding consumes the Golgi membrane leading to the disassembly of the Golgi apparatus while excess vesicle fusion cause enlargement of the Golgi apparatus with slower transport out of the secretory proteins. How the input and output is balanced is not well understood while it is apparent that the control of vesicle fusion has to be a key. After the vesicles are budded from the donor membrane, they move to the target membrane mediated by diffusion or motor dependent transport. The initial physical link between a vesicle and a target membrane is occurred when a vesicle is tethered by (a) tethering factor(s), such as coiled-coil proteins or multimeric tethering complexes (Lupashin and Sztul, 2005; Cai *et al.*, 2007). The fusion of vesicles with Golgi membrane is then promoted by membrane-bound proteins known as SNAREs (soluble N-ethylmaleimide-sensitive factor attachment protein receptor).

The vesicle budding/fusion may also be mediated by Yip1p, a YIP domain family protein, which was first identified in the *Saccharomyces Cerevisiae.* This protein interacts with Ypt1p and Ypt31p, the yeast homologs of mammalian Rab1 and Rab11, respectively (Yang *et al*., 1998). Yip1p forms a complex with Yif1p and Yos1p. This complex is found in ER-derived COPII transport vesicles and thought to function in the vesicle docking/fusion at

the Golgi apparatus. Yip1p-Yif1p complex interacts ER to Golgi SNAREs Bos1p and Sec22p (Barrowman *et al.*, 2003; Heidtman *et al*., 2003; Heidtman *et al*., 2005). Nine human family members of the Yip1p/Yif1p family (YIPF) were identified (Shakoori *et al*., 2003). YIPF5 and YIPF3 were reported to interact with YIF1A and YIPF4, respectively. They localize in the ERGIC and the Golgi apparatus and maintain the Golgi structure (Yoshida *et al*., 2008; Tanimoto *et al*., 2011). YIPF1, YIPF2 and YIPF 6 are other family members of Yip domain family protein in human but the localization and their function were not determined. Therefore, I decided to analyze the localization and function of these proteins to explore their function in the maintenance of the Golgi structure. The results of this analysis was described and discussed in ***Chapter II.***

Chapter I. The disassembly of Golgi apparatus and its mediated factors under acidic extracellular pH condition

The study in this chapter was published on Experimental Cell Research 328, p325-339 in 2014 as “Low cytoplasmic pH reduces ER-Golgi trafficking and induces disassembly of the Golgi apparatus” by Soonthornsit , J., Yamaguchi, Y., Tamura, D., Ishida, R., Nakakoji, Y., Osako, S., Yamamoto, A., Nakamura, N.

Introduction

In mammalian cells, Golgi apparatus has a stacked cisternal structure and the Golgi stacks are laterally connected to form a continuous ribbon-like structure in most of higher eukaryote cells (Shorter and Warren, 2002). The reason of this has not been well understood, but it is thought to relate with the polarized secretion and transport of membrane proteins. The Golgi structure is thought to be necessary for driving the normal Golgi function. The Golgi morphological changes often lead to the abnormalities of Golgi function. For example, the cisternae are very thin and stacks show a circular structure when the protein synthesis is blocked (Taylor *et al.*, 1997). The decrease of the tensile force for extending Golgi ribbon of GOLPH3/MYO18A/F-actin perturbed Golgi trafficking and morphology (Dippold *et al*., 2009). BFA drug treatment causes the Golgi disassembly, the newly synthesized protein appeared to be retained and Golgi enzymes are redistributed to ER (Klausner *et al.*, 1992). Golgi ribbon were broken down into mini-stacks in many neurological diseases including Parkinson's disease, which is caused by phosphorylation of Golgi structural proteins (Joshi *et al*., 2014). These observations indicated that the maintenance of the Golgi structure is supported by many factors localized on the Golgi apparatus.

The Golgi structure is maintained by highly dynamic of vesicular and tubular carriers. The docking of vesicles on Golgi membrane is mediated by many factors, including Golgi matrix proteins that are involved in the regulation of membranes traffic and maintenance of Golgi morphology (Martinez-Alonso and Tomas, 2013). During cell division, Golgi apparatus undergoes cisternal unstacking induced by mitotic phosphorylation of tethering proteins called Golgi matrix proteins, GRASPs and GM130. After the exit from the mitosis the Golgi apparatus is restacked by the re-activation of tethering proteins that mediate Golgi membrane and vesicle fusion. (Lowe *et al.*, 1998; Tang and Wang, 2013). In interphase cells, the inhibition of ER to Golgi transport cause the fragmentation of the Golgi apparatus

concomitant with the relocalization of the Golgi resident proteins to the ER while the Golgi matrix proteins are retained in punctate structures scattered in the cytosol (Yoshimura *et al.*, 2004).

Tubular structures are frequently found to emanate from the Golgi apparatus, however, the molecular machinery of Golgi tubule formation has not clearly understood. The formation of membrane tubules is thought to require a high degree of transmembrane lipid asymmetry, which can be produced by special protein machinery and metabolism. Phospholipase A_2 (PLA_2) enzymes cleave fatty acids at the sn-2 position of glycerol and phospholipids, which generates a free fatty acid and a lysophospholipid, and generate the membrane curvature (Bechler *et al*., 2012). PLA_2s are reported to play roles in Golgi tubule formation and maintenance of the Golgi structure (Bechler *et al*., 2011).

The position of Golgi apparatus and the movement of transport carriers around Golgi are regulated by cytoskeleton (Brown *et al*., 2014; Ho *et al.*, 1989). Nocodazole-induced microtubule depolymerization induces a breakdown of the Golgi ribbon into mini-stacks. This process is reversible and the mini-stacks are reformed into a normal Golgi ribbon after the washout of the drug (Ho *et al*., 1989).

In my laboratory, it was found that Golgi apparatus quickly disassembled in a low pH medium. In this chapter, the analyses of the mechanism of the low pH induced Golgi disassembly are described.

Results

The reversible disassembly of Golgi apparatus induced by low pH medium

Golgi apparatus was quickly disassembled when HeLa cells were incubated in a low pH medium (pH 6.3). GM130, *cis*-Golgi marker, was markedly disassembled and found in tubular structures at 15 minutes. The Golgi was completely fragmented within 30 minutes and *cis*-Golgi was not observed as a ribbon-like structure anymore. The *cis*-Golgi was completely dispersed toward the cell periphery within 60 minutes of the low pH treatment. The similar disassembly was also observed for giantin, *media-/trans*-Golgi marker. Giantin showed complete fragmentation and dispersal within 60 minutes (Fig. 1A left panels). It was noted that the disassembly of the *medial/trans* marker was significantly slower compared with *cis*-Golgi marker (discussed later again). To determine whether the Golgi disassembly was reversible, the medium was changed to the control pH (pH 7.3) after 60 minutes of low pH medium incubation. The dispersed Golgi fragments started to reassemble into larger fragments at 15 minutes, then those were further accumulated around juxtanulclear position and reformed a ribbon-like structure at 30-60 minutes, and completely reassembled within 120 minutes (Fig. 1A right panels). This result indicated that disassembly of the Golgi apparatus induced by the low pH medium was a reversible phenomenon.

The response of the Golgi apparatus under low pH condition was not specific to HeLa cells, the Golgi disassembly was also found in HEK293 cells. The disassembly phenotype was similar to HeLa cells so that *cis*- and *media-/trans*-Golgi marker were disassembled after 30 minutes and reassembled within 2 hours (Fig. 1B).

All Golgi compartments were disassembled and *cis*-Golgi was disassembled prior to the other compartment.

It was found that the *cis*-Golgi (GM130) responded to the low pH treatment quickly and was significantly separated from the *medial*- (GlcNAc-T1-GFP), *trans*-Golgi (GalT-RFP) and TGN (TGN46) compartments after the dispersal. Tubular structures of *cis*-Golgi were observed within 15 minutes after low pH medium incubation, then the *cis*-Golgi tubules were gradually decreased and smaller fragments were continuously increased at the cell periphery within 30 minutes. On the other hand, the *medial*-, *trans*-Golgi and TGN were disassembled in a slower kinetics, and those markers were clearly colocalized in larger fragments around juxtanuclear position (Fig. 2). Tubular structures were not found for these markers. This result suggested that *cis*-Golgi was more sensitive to low pH treatment and disassembled prior to the other part of the Golgi apparatus.

The ultrastructural observation was performed using electron microscopy. In control pH, Golgi apparatus was observed as a stacked cisternal structure surrounded with vesicles around the juxtanuclear position. On the other hand, the Golgi stack was not found after the low pH incubation (Fig. 3, left panel). Only cluster of inflated vesicles were observed in the juxtanuclear position where the Golgi stack were located in control condition. This result indicated that the whole Golgi stack disassembled by the low pH treatment.

Anterograde transport was delayed under the low pH condition.

To investigate the function of Golgi apparatus after the low pH-induced Golgi disassembly, the transport of vesicular stomatitis virus glycoprotein of the tsO45 mutant (VSV-G tsO45) fused with GFP as a membrane protein marker was used for monitoring the anterograde transport. VSV-G (tsO45)-GFP is accumulated in the ER at restricted temperature (39.5˚C) and is permitted to transport out of the ER to plasma membrane at

permissive temperature (32˚C) (Presley *et al*., 1997). HeLa cells were allowed to express VSV-G (tsO45)-GFP at 39.5˚C overnight in a control pH medium, and then were incubated in control pH or low pH medium for 1 hour at 39.5˚C. The temperature was shifted to 32˚C in the presence of cyclohexamide to inhibit a new protein synthesis in the ER. The transport of VSV-G (tsO45)-GFP protein was observed in each time point as described in Fig. 4.

In control medium, VSV-G (tsO45)-GFP protein was appeared in cytoplasmic reticular structure and nuclear envelope, a typical ER pattern, before the temperature shift. After the temperature shift, VSV-G (tsO45)-GFP protein partly appeared as a juxtanuclear ribbon like structure and colocalized with GM130 at 15 minutes indicating the delivery to the Golgi apparatus. At 45 minutes, VSV-G (tsO45)-GFP mostly colocalized with GM130 and partially presented at the plasma membrane while reticular structure and nuclear envelope was disappeared, indicating that most of VSV-G (tsO45)-GFP was transported out of ER. After 2 hours, it was mostly transported to plasma membrane and completely cleared from Golgi apparatus at 4 hours after the temperature shift (Fig. 4, upper gallery).

In low pH medium, VSV-G (tsO45)-GFP was also appeared in the ER before the temperature shift. However, a VSV-G (tsO45)-GFP was mostly remained in the ER after 15 minutes, and only partially colocalized with GM130 at 45 minutes. The transport of VSV-G (tsO45)-GFP to the plasma membrane was significantly delayed and only partial plasma membrane localization was observed after 4 hours. This result suggested the anterograde transport of VSV-G (tsO45)-GFP was strongly inhibited under the low pH condition (Fig. 4, lower gallery).

No effect in actin structure under low pH treatment.

The maintenance of the Golgi morphology also involves cytoskeleton (Ho *et al*., 1989; Dippold *et al*., 2009). Therefore, I investigated the structure of the actin filaments using

fluorescent conjugates of phalloidin (FITC-phalloidin) after the incubation with a control or low pH medium for 30 minutes. In Fig. 5, no significant effect in actin filament structure was observed between a control and low pH condition. This result indicated that the disassembly of Golgi apparatus was not mediated by the disruption of actin filaments.

PLA_2 inhibitors protected Golgi disassembly induced by low pH treatment.

Cis-Golgi tubules appeared in early stage of Golgi disassembly after low pH treatment. Then, *cis*-Golgi tubules gradually decreased and the *cis*-Golgi fragments continually increased until the complete disassembly after 30 minutes. Therefore, it was suggested that these tubules might mediate the disassembly of the Golgi apparatus under the low pH condition. I focused on a group of phospholipase A_2 (PLA_2)s because they were reported to be involved in the formation of membrane tubules from Golgi apparatus (Bechler *et al*., 2012). HeLa cells were treated with a control or low pH medium in the presence of PLA_2 inhibitors, NO-RS-082 (ONO), bromoenol lactone (BEL), cPLA2α inhibitor (Pyrrolidine derivative), arachidonyl trifluoromethyl ketone (AACOCF3) or methyl arachidonyl fluorophosphonate (MAFP) for 30 minutes fixed and analyzed by immunofluorescence staining. The results showed that only ONO and BEL significantly inhibited the Golgi disassembly induced by low pH treatment. The Golgi ribbon was clearly observed in juxtanuclear position at higher concentration of the drugs (Fig 6A). In contrast, Golgi apparatus was completely fragmented in the presence of cPLA2α inhibitor, MAFP or AACOCF3. Notably, GM130 diffused over the cytoplasm at high concentration of AACOCF3 in control and low pH treated cells (Fig. 6B). The mechanism of the diffusion of GM130 under this condition is unclear and has to be analyzed in future. To confirm the protective effect of ONO and BEL, the number of the cells that showed the ribbon-like structure of the Golgi apparatus (cells with protective effect) were counted (Fig. 7A). As

shown in Fig. 7B, the clear inhibition was found more than 40% of cells at 540 μM and 80 μM for ONO and BEL, respectively. This inhibition was clearer and stronger at higher concentration of the drugs. These results suggested that PLA_2 promotes the Golgi disassembly under low pH condition.

The Rab1 suppressed the Golgi disassembly and dispersal under low pH treatment

Rab proteins are major regulators of membrane trafficking and essential for maintenance of Golgi structure via the regulation of vesicle tethering, and fusion (Schwartz *et al*., 2007; Liu and Storrie, 2012). Especially, Rab1 was reported to be involved in ER-to-Golgi and intra Golgi transport, and also in the maintenance of Golgi structure (Wilson *et al*., 1994). Therefore, involvement of Rab1 in the Golgi disassembly under low pH condition was analyzed. HA-tagged wild type Rab1 (HA-Rab1) was expressed in HeLa cells for 24 hours and treated with low pH. As shown in Fig. 8, the Golgi apparatus appeared in smaller fragments and more dispersed toward the cell periphery in non-expressing cells. In contrast, the Golgi apparatus was slightly fragmented but mostly in a ribbon-like structure accumulated at juxtanuclear position by HA-Rab1 overexpression. This result suggested that Rab1 protected the Golgi apparatus from the disassembly induced by low pH medium.

The overexpression of Rab1 did not rescue anterograde transport under low pH treatment

According to the results in Fig.4, low pH treatment induced the disassembly of the Golgi apparatus and significantly delayed VSV-G (tsO45)-GFP transport from ER to plasma membrane. Because overexpression of HA-Rab1 suppressed the disassembly of Golgi apparatus (Fig. 8), the overexpression of HA-Rab1 may rescue the VSV-G (tsO45)-GFP transport in a low pH medium. The exogenous HA-Rab1 was transfected into HeLa cells, and

then allowed to expressed VSV-G (tsO45)-GFP at 39.5˚C overnight in a control pH medium, and then cells were incubated in control pH or low pH medium for 1 hour at 39.5˚C. The temperature was shifted to 32˚C in the presence of cycloheximide and incubated for indicated time. Similar to the results described above (Fig. 4), VSV-G (tsO45)-GFP was transported to the Golgi apparatus after 15 minutes and reached to the plasma membrane after 45 minutes when cells were incubated with control pH medium. No difference was observed in Rab1 expressing and non-expressing cells (Fig. 9, upper gallery). Similar to the previous result (Fig. 4), the low pH treatment strongly reduced the transport of VSV-G (tsO45)-GFP. Again, no difference was observed for the transport of VSV-G (tsO45)-GFP in Rab1 expressing and non-expressing cells (Fig. 9, lower gallery). This result indicated that the overexpression of HA-Rab1 could not rescue VSV-G (tsO45)-GFP transport under the low pH condition.

High temperature negated the Rab1 function for suppressing the Golgi disassembly

Next, I tried to determine why HA-Rab1 overexpression could not rescue the transport of VSV-G (tsO45)-GFP. In VSV-G (tsO45)-GFP transport assay, I found that the Golgi disassembly was not protected from the disassembly by the overexpression of HA-Rab1 as described above (Fig. 9). It was possible that, the temperature may affect the function for Rab1. To investigate this, the structure of the Golgi apparatus was analyzed in different temperatures. HeLa cells were allowed to express HA-Rab1 24 hour and the cells were incubated in three different temperature conditions, 32˚C, 37˚C and 39.5˚C for 1 hour, and finally, the cells were treated with a control pH and a low pH medium at 32˚C, 37˚C and 39.5˚C for 30 minutes.

In control pH, the Golgi apparatus showed typical ribbon-like structure at 32˚C and 37˚C and the expression of HA-Rab1 did not affect this structure (Fig. 10, upper gallery) similar to the result described above (Fig. 8, upper panels). Interestingly, Golgi apparatus was

slightly fragmented in non-expressing cells at 39.5˚C. While normal Golgi ribbon was observed in HA-Rab1-expressing cells.

Similar to the results described above (Fig. 8), the expression of HA-Rab1 clearly suppressed the disassembly of the Golgi apparatus by the low pH treatment at 37˚C and 32˚C. On the other hand, the expression of HA-Rab1 did not inhibit the Golgi disassembly at 39.5˚C in low pH treated cells although the careful observation revealed that the dispersal of the Golgi apparatus was incomplete in the HA-Rab1 expressing cells (Fig. 10, lower gallery). These results strongly suggested that the high temperature incubation negated the effect of Rab1 and this is the reason why Rab1 expression did not rescue the transport of VSV-G (tsO45)-GFP.

Discussions

Extracellular acidification is found in a number of diseases such as cancer, ischemia and inflammation (Vaupel *et al*., 1989). An acidic extracellular pH of tumor microenvironment, which facilitates the cell invasion of metastatic breast cancer cells, induces a low intracellular pH results in a relocalization of lysosomes from the perinuclear region to the cell periphery (Glunde *et al*., 2003). The low cytoplasmic pH has multiple effects to intracellular organelles. For instance, an acidic pH induces DNA damage via a topoisomerase II (TOP2) isozymes dependent pathway and trigger tumor cell death (Xiao *et al*., 2003). It also enhances VEGF transcription leading to increased VEGF production, which induces angiogenesis to promote tumor growth (Xu *et al*., 2002). The low pH changes the redistribution of late endosomes and lysosomes towards the plus ends of the microtubules (Heuser, 1989; Parton *et al*., 1991). Here, I found that Golgi apparatus was completely disassembled within 30 minutes after the low pH medium (pH6.3) incubation and it was reassembled to form a ribbon-like structure within 2 hours after replacing with a control pH medium in both HeLa and HEK293 cells (Fig. 1). The similar response is found in other cell lines such as normal rat kidney (NRK), PC12 cells and Chinese hamster ovary (CHO) cells (Soonthornsit *et al*., 2014). The first observation of Golgi disassembly in low pH medium was reported in hepatoma cells after prolonged incubation (Yoshida *et al*., 1999). These findings suggested that the reversible disassembly of the Golgi apparatus induced by a low pH condition was not cell type-specific, while the sensitivity of Golgi disassembly was depended on the cell type. We have found that low pH medium reduced the cytoplasmic pH but not the luminal pH of Golgi apparatus suggesting that the low cytoplasmic pH trigger the disassembly of the Golgi apparatus (Soonthornsit *et al.*, 2014).

The ultrastructural observation showed that the low pH treatment induced the disassembly of the whole Golgi apparatus (Fig. 3). *Cis*-Golgi was separated from *medial*-

/*trans*-Golgi and TGN. The *cis*-Golgi was disassembled prior to other Golgi compartments and tubular structures were appeared from the *cis*-Golgi in early stage of the low pH incubation. Then, *cis*-Golgi tubules were gradually decreased, while *cis*-Golgi fragments were increased in later stage of incubation. The tubular structures were clearly observed in live cell imaging. They were emanated from *cis*-Golgi leading to complete disassembly of *cis*-Golgi compartment (Soonthornsit *et al*, 2014). In contrast, *medial*-/ *trans*-Golgi and TGN did not show tubular structures (Fig. 1 and 2). This phenotype was different from BFA- and nocodazole-induced Golgi disassembly. BFA causes a rapid and dramatic redistribution of Golgi residential enzymes to the ER. Clear Golgi tubules emanating from *medial*-/ *trans*-Golgi and TGN were observed at early stage and ER-like structure were observed at late stage after BFA treatment (Lippincott-Schwartz *et al*., 1898; Klausner *et al.*, 1992). Nocodazole depolymerizes microtubules and mediates the disassembly of the Golgi apparatus while *cis*-, *medial*- and *trans*-Golgi compartments associate in same punctate structures, which are found to be a mini-Golgi stack (Ho *et al*., 1989). No tubular structure was formed by nocodazole treatment.

The low pH medium treatment significantly reduced anterograde transport of VSV-G (tsO45)-GFP in both ER-to-Golgi and Golgi-to plasma membrane level (Fig. 4). This result is similar to the previous report that VSV-G protein transport was delayed under low pH. VSV-G was accumulated in TGN, which thought to be caused by the inhibition of vesicular budding at TGN (Cosson *et al*., 1989).

The maintenance of Golgi structure was associated with cytoskeleton, including microtubules and actin filaments. The disruption of microtubule such as the nocodazole treatment causes Golgi mini-stack formation. However, the structure of microtubules was not changed by the low pH treatment (Soonthornsit *et al*, 2014). In addition, no significant effect in actin filament structure was observed (Fig. 5). Therefore, it was strongly suggested that

Golgi disassembly induced by a low pH medium was not mediated by the direct disruption of microtubules or microfilaments. Instead, it is probable that motor proteins are involved in the disassembly. The localization of Golgi apparatus at juxtanuclear position is regulated by dynein and kinesin, which move along microtubules. It is well known that dynein pulls Golgi apparatus to the minus ends and anchors the Golgi apparatus at centrosomes. Kinesin pulls Golgi apparatus to the plus ends of microtubules toward the cell periphery. There was a report that low cytoplasmic pH induced microtubule-dependent redistribution of late endosomes and lysosomes, which were thought that the activity of kinesin would be over dynein (Parton *et al*., 1991). There is a possibility that the pulling force of dynein might be lower than kinesin in low pH condition. Similar to endosomes and lysosomes, the Golgi ribbons may be pulled toward the cell periphery leading to the fragmentation and dispersal of the Golgi apparatus dependent of the microtubules. This possibility has to be evaluated in future.

Structure of the Golgi apparatus is maintained by the balance of input and output of vesicular and tubular elements. Tubules form extensive network and facilitate intra-Golgi transport and transport between the Golgi apparatus and others organelles such as ER and endosomes (Martinez-Alonso and Tomas, 2013). During the Golgi disassembly by low pH treatment, *cis*-Golgi tubules appeared in tubular structures within 15 minutes and the tubular structures were gradually decreased at later time points and, concomitantly, *cis*-Golgi fragments were increased (Figs. 1 and 2). These tubules were found at peripheral cytoplasmic region and showed dynamic movement by live cell imaging (Soonthornsit *et al*, 2014). These results suggested that the Golgi disassembly induced by the low pH treatment was mediated by the formation of tubules from the *cis*-Golgi. There have been the reports that the formation of membrane tubules required a high degree of transmembrane lipid asymmetry, which was mediated by phospholipase enzymes. So far, at least three phospholipase A_2 (PLA_2),

including Ca^{2+}-dependent PLA_2-α (cPLA2α), Ca^{2+}-independent PLA_2-β (iPLA2-β) and platelet-activating factor acetylhydrolase Ib (PAFAH Ib), were reported to induce tubules form the Golgi membrane (Bechler *et al*., 2011; Martinez-Alonso and Tomas, 2013). The PLA_2 antagonists, which were used in this study, have multiple targets. ONO inhibits $cPLA_2$α, $iPLA_2$-β and PAFAH Ib. BEL inhibits $iPLA_2$-β and PAFAH Ib. CPLA2α inhibitor inhibits $cPLA_2$α. AACOCF3 and MAFP inhibit $cPLA_2$α and $iPLA_2$-β (Bechler *et al*, 2012). As shown in Fig. 6, only ONO and BEL showed clear inhibition of the Golgi disassembly. Therefore, it is most probable that platelet-activating factor acetylhydrolase (PAFAH Ib) is responsible for the disassembly of the Golgi apparatus induced by the low pH treatment. PAFAH Ib consists of two catalytic subunits, α1 and α2, and one the dynein regulator lissencephaly1 (LIS1) subunits. It was reported that PAFAH Ib induced tubules from the Golgi membrane. The knockdown of α1 and α2 subunits of PAFAH Ib induces fragmentation of the Golgi ribbon and inhibits tubule-mediated Golgi reassembly during recovery from BFA (Bechler *et al*, 2010). Therefore, it is possible that the low pH treatment altered the activity of PAFAH Ib inducing tubule formation from the Golgi apparatus leading to the disassembly of the Golgi apparatus.

Rab family GTPases are essential regulators in vesicular tethering and fusion for maintaining the Golgi structure. It was found that the overexpression of Rab1 suppressed the Golgi disassembly induced by a low pH treatment (Fig. 8). The inhibition was also found by the expression of Rab41 (Soonthornsit *et al*, 2014), which is also reported to be required for the maintenance of the ribbon-like structure of the Golgi apparatus (Liu *et al*., 2013). These results suggested that at least Rab1 and Rab41 protect the Golgi apparatus from the disassembly induced by the low pH treatment. It is known that Rab1 is required for the tethering of COPII vesicle and Golgi maintenance (Haas *et al*., 2007). Therefore, it is possible that Rab1 has less activity in low cytoplasmic pH while the overexpression of Rab1

compensated the vesicle tethering / fusion to the Golgi membrane leading to the suppression of Golgi disassembly.

The over expression of Rab1 could not rescue the anterograde transport under the low pH treatment (Fig. 9). This was shown to be correlated with the fragmentation of the Golgi apparatus at high temperature (Fig. 10). It is most probable that vesicle tethering / fusion at the Golgi apparatus mediated by Rab1 is compromised by the low pH treatment and also by high temperature treatment leading to the fragmentation and dispersal of the Golgi apparatus. The relationship of the functions of Rab1 and PLA_2 in low cytoplasmic pH or/and high temperature condition should be investigated in future.

Chapter II. The localization of YIPF1, YIPF2 and YIPF6 and their functions

Introduction

Rab/Ypt GTPase family proteins are known to be involved in vesicular trafficking, which mediates intracellular transport, secretion, and endocytosis (Schmitt *et al*., 1986; Salminen and Novick, 1987; Bucci *et al*., 1995; Bucci *et al*., 2000). In yeast, the mutation of Ypt1 blocks in ER to *cis*-Golgi and *cis*- to *medial*-Golgi transport (Jedd *et al*., 1995). On the other hand, the mutation of Ypt31p and Ypt32p block the protein export from the late exocytic pathway (Jedd *et al*., 1997). Yip1p was identified as a protein, which interact and facilitate Ypt1p and Ypt31p function. Yip1p is an integral membrane protein that localizes in Golgi apparatus in steady state. The Yip1p mutation inhibits protein transport at early stage in biosynthetic pathway and impairs the glycosylation process, which is essential for cell viability (Yang *et al*., 1998). Yip1p forms a heteromeric complex with another multi-spanning integral membrane protein termed Yif1p (Matern *et al*., 2000). Yip1p-Yif1p complex mediate the COPII vesicle budding from the ER and/or fusion to the Golgi membrane (Barrowman *et al*., 2003; Heidtman *et al*., 2003).

Nine human family members of the Yip1p/Yif1p family (YIPF) were identified and found to localize in ER and Golgi apparatus. The proteins have five transmembrane segments and expose the *N*-terminus to cytoplasm and the *C*-terminus to the lumen. Similar to Yip1p and Yif1p in budding yeast, YIPF5 (Yip1A) and YIF1A, the human orthologue of Yip1p and Yif1p, respectively, form a complex. In addition, YIPF4 and YIPF3, a homologue of YIPF5 and YIF1A, respectively, form a complex. These interactions are mediated by their transmembrane regions (Shakoori *et al*., 2003). Moreover, the loss of YIPF5 and YIPF3 reduced the amount of their partners, suggesting that they are essential for stabilizing their partners. The YIPF4-YIPF3 complex is concentrated in the *cis*-Golgi compartment and involved in the maintenance of Golgi structure (Tanimoto *et al*., 2011). The YIPF5-YIF1A complex localizes in ERGIC and some in *cis*-Golgi compartment (Yoshida *et al*., 2008). The

knockdown of YIPF5 delays the retrograde transport of Shiga toxin (Kano *et al*., 2009) and anterograde transport of VSVG protein. Moreover, YIPF5 knockdown was reported to induce the loss of the peripheral tubular ER network, the clustering of ER membranes and the slowing down of the protein export (Dykstra *et al*., 2010). These results indicated that Yip1p/Yif1p family proteins play some roles in vesicular trafficking and directly or indirectly involved in the maintenance of the structure of Golgi apparatus and the ER. Because yeast Yip1p was shown to interact with Ypt proteins, it is a probable that human YIPF proteins interact with Rab proteins to regulate the vesicular transport.

YIPF1, YIPF2 and YIPF6 are Yip1p/Yif1p family members and were reported to localize in Golgi apparatus (Shakoori *et al*., 2003). YIPF1 and YIPF2 are human homologues of Yif1p, and YIPF6 is a human homologue of Yip1p. Using Yeast two hybrid analysis, YIPF1 and YIPF2 showed strong interaction with YIPF6 (Shakoori *et al*., 2003), however, their precise localization and their roles have not been analyzed. In this chapter, the analysis of the precise location and their function are described.

Results

YIPF1, YIPF2 and YIPF6 localized in *medial-*, *trans*-Golgi and TGN

To analyze the precise localization of YIPF1, YIPF2 and YIPF6, affinity purified rabbit polyclonal antibodies for these proteins were produced and used for double immunofluorescence staining. GM130 and TGN46 were used for the markers of *cis*-Golgi, and TGN, respectively and GlcNAc-T1-RFP, GALT1-RFP were transiently expressed in HeLa cells and used for *medial*- and *trans*-Golgi markers.

All markers appeared as a ribbon-like structure at juxtanuclear position. The endogenous YIPF1, YIPF2 and YIPF6 also showed a ribbon-like structure and were partially overlapped with GlcNAc-T1-RFP, GalT-RFP and TGN46. In contrast, All YIPFs were clearly separated with GM130, *cis*-Golgi marker (Fig. 11). These results suggested that YIPF1, YIPF2 and YIPF6 mainly localized in *medial-*, *trans*-Golgi and TGN.

To confirm the localization of YIPF1, YIPF2 and YIPF6, the cells were subjected to the low pH treatment, in which *cis*-Golgi (GM130) was disassembled prior to the other Golgi compartments (Fig. 12). After 15 minutes of the low pH treatment, *cis*-Golgi was appeared in both tubular and punctate structures. On the other hand, *medial-*, *trans*-Golgi and TGN Golgi compartments were disassembled slower appearing in larger fragments without tubular structures. In low pH treatment, YIPF1, YIPF2 and YIPF6 clearly overlaid with the GlcNAc-T1-RFP, GalT-RFP and TGN46, which were separated from GM130. These results confirmed that YIPF1, YIPF2 and YIPF6 were mainly localized in *medial-*, *trans*-Golgi and TGN.

Knockdown of YIPF1, YIPF2 and YIPF6

To investigate the function of YIPF1, YIPF2 and YIPF6, the knockdown of these proteins were performed. HeLa cells were transfected with siRNA targeting for YIPF1, YIPF2 and YIPF6 and incubated for 3 days. The cells were then analyzed by western blotting to quantitate the efficiency of the reduction. As shown in Fig. 13, YIPF1, YIPF2 and YIPF6 were successfully knocked down to less than 10%. Strikingly, YIPF1 and YIPF2 were strongly reduced by the knockdown of YIPF6. In contrast, knockdown of YIPF1 did not significantly affect the amount of YIPF6. The amount of YIPF6 was slightly reduced by YIPF2 knockdown but not to the level found by YIPF6 knockdown. Double knockdown of YIPF1 and YIPF2 did not further reduce the amount of YIPF6 (Fig. 13, F1+2KD). These results suggested that YIPF6 was important for stability of YIPF1 and YIPF2 but not vice versa.

YIPF1, YIPF2 and YIPF6 knockdown reduced the disassembly of *medial-*, *trans*-Golgi and TGN induced by the low pH treatment

After confirming the success of the knockdown of YIPF1, YIPF2 and YIPF6, whether these three YIPFs are involved in the maintenance of the Golgi structure was analyzed. YIPF1, YIPF2 and YIPF6 were singly or doubly knocked down in HeLa cells and subjected to the immunofluorescence analysis. As a result, the reduction of YIPFs did not show obvious effect on the Golgi structure (Fig. 14A). This result suggested that the reduction of YIPF1, YIPF2 and YIPF6 did not affect the Golgi structure in steady state.

Although the knockdown of YIPF1, YIPF2 and YIPF6 showed least effect on the morphology of the Golgi apparatus, it may be involved in the transport pathway, which is less active in normal condition. Therefore, we sought to activate transport pathway that is less active. Obviously, the low pH treatment described in Chapter I is a good candidate condition

to try. Thus, HeLa cells were knocked down for YIPF1, YIPF2 and YIPF6 and incubated in a low pH medium for 15 and 30 minutes. In control cells, GM130 appeared in tubular and punctate structures at juxtanuclear position and cell periphery at 15 minutes, and it was dispersed more to the cytoplasm at 30 minutes. Giantin and TGN46 presented in puncta in the juxtanuclear position at 15 minutes, and they redistributed toward the cell periphery at 30 minutes (Fig. 14B). After the single knockdown of YIPF1, YIPF2 or YIPF6 and also after the double knockdown of YIPF1 and YIPF2, the disassembly of *medial-/trans*- Golgi and TGN by the low pH treatment was significantly inhibited. Giantin and TGN46 were remained in a ribbon-like structure at 15 minutes and, they were in bigger fragments and remained at the juxtanuclear position less dispersing toward the periphery of the cells at 30 minutes (Fig. 14B). To confirm the significance of this effect, the cells showing intact Golgi and fragmented Golgi were categorized as shown in Fig. 15A and quantitated. As shown in Fig. 15B, giantin and TGN46 was found in intact Golgi in more than 60% of the cells, in which YIPF1, YIPF2 were singly knocked down or doubly knocked down, after 15 minutes of low pH treatment. Similarly, giantin and TGN46 was found in intact Golgi in about 50% of cells, in which YIPF6 was knocked down at the same time point. Giantin and TGN46 was found in intact Golgi in more than 20% of the cells after 30 minutes of low pH in treatment, in which YIPF2 knocked down cells irrespective the simultaneous knock down of YIPF1, while no significant effect was found in other knockdown conditions. Interestingly, no significant effect was found for GM130 in any knockdown conditions. These results strongly suggested that YIPF1, YIPF2 and YIPF6 delayed the low pH induced disassembly of *medial-/trans*-Golgi and TGN but not the *cis*-Golgi.

YIPF1 and YIPF2 knockdown reduced the glycoprotein production

Although the structure of the Golgi apparatus was not significantly affected at the normal condition, the significant delay of the Golgi dispersal after the low pH treatment invoked the possibility that the function of the Golgi apparatus was somewhat compromised after the knockdown of YIPF1, YIPF2 or YIPF6. Intriguingly, there was a report suggesting that YIPF6 is involved in the mucin secretion at the intestine (Brandl *et al*., 2012). To evaluate this possibility, the effect of the knockdown of YIPF proteins on the production of glycoprotein was investigated in a goblet cell line, HT-29, which produces higher amount of mucins.

As shown in Fig. 16A and B, the knockdown of YIPFs were successful and the pattern of the reduction of YIPF proteins were similar as in the case of HeLa cells although the knockdown efficiency was slightly lower. The periodic acid-schiff (PAS) reaction was performed to visualize the glycoprotein. As shown in Fig. 15C, clear PAS staining was observed for all the conditions. However, careful observation revealed that the staining was fainter in YIPF1 or YIPF2 knockdown cells. To substantiate the difference in the staining, average density of the staining was quantitated by an image analysis as described in Materials and Methods. As shown in Fig. 16D, the average staining density was lower in YIPF1 or YIPF2 knockdown cells. Similar reduction was also observed in doubly knocked down cells for YIPF1 and YIPF2. Curiously, the average staining density was not significantly reduced in YIPF6 knocked down cells.

Discussions

It was reported that the exogenously expressed YIPF1, YIPF2 and YIPF6 localized on Golgi apparatus (Shakoori *et al*., 2003). Consistent with this report, the endogenous YIPF1, YIPF2 and YIPF6 mainly localized in *medial-*, *trans*-Golgi and TGN (Fig. 11). They overlapped and behaved in similar way with *medial-*, *trans*-Golgi and TGN marker proteins during the Golgi disassembly induced by low pH treatment (Fig. 12). Yeast two-hybrid analysis showed YIPF1 and YIPF2 strongly interacted with YIPF6 (Shakoori *et al*., 2003). Accordingly, YIPF1, YIPF2 and YIPF6 formed a complex in HeLa cells (unpublished results). Here, it was found that the stability of YIPF1 and YIPF2 was dependent on the presence of YIPF6 (Fig. 13). These results strongly suggested that YIPF1, YIPF2 and YIPF6 are the partners and forms a complex in *medial-*, *trans*-Golgi and TGN.

It was reported that YIPF5-YIF1A and YIPF4-YIPF3 complex localized in ERGIC and *cis*-Golgi compartment, respectively, and they were involved the maintenance of Golgi structure (Tanimoto *et al*., 2011; Yoshida *et al*., 2008). On the other hand, the knockdown of YIPF 1, YIPF2 and YIPF6 did not shown any significant effect on Golgi structure in normal culture condition. However, the disassembly of *medial-*, *trans*-Golgi and TGN under the low pH treatment was delayed by the knockdown either of these three YIPFs (Fig. 14). These results suggested that YIPF1, YIPF2 and YIPF6 functions to promote the disassembly of the Golgi apparatus. It is possible that YIPF1, YIPF2 and YIPF6 promote vesicle budding form the *medial-*, *trans*-Golgi and TGN under the low pH condition.

The knockdown of YIPF2 delayed the disassembly induced by the low pH treatment in HeLa cells (Fig. 15). Accordingly, the glycosylated proteins in the cells were significantly reduced in YIPF2 knocked down HT29 cells (Fig. 15). Similar effect was found for YIPF1. However, the delaying effect for the low pH induced Golgi disassembly was weaker compared with YIPF2 (Fig. 15B, Low pH 30 min). Accordingly, the reduction of the

glycosylated proteins in the cells were slightly less in YIPF1 knocked down cells. The delaying effect for the low pH induced Golgi disassembly was further weak compared with YIPF1 and YIPF2. Accordingly, the glycosylated proteins in the cells were not significantly reduced in YIPF6 knocked down HT29 cells (Fig. 16). This result appeared to contradict with the report that the splicing mutation of YIPF6, which lacked transmembrane domain, caused the reduction of mucin content in Goblet cell and induces spontaneous intestinal inflammation in mice (Brandl *et al*., 2012). However, this mutant expresses a *N*-terminal cytosolic domain of YIPF6 as a result of the mutation. Therefore, the condition was different from our knockdown of YIPF6. The cytosolic domain of YIPF6 may interfere with a normal function of YIPF1/YIPF2 –YIPF6 complex exaggerating the normal function of the Golgi apparatus resulting in the defect in the mucin secretion. The effect of the expression of the cytosolic domain of YIPF6 is being analyzed in our laboratory to evaluate this possibility. The analysis whether YIPF1 and YIPF2 were reduced in this YIPF6 mutant may be necessary to resolve the discrepancy.

Materials and Methods

Cell culture and pH conditioned media

HeLa cells were grown in Dulbecco's modified Eagle's medium-high glucose (DMEM) (Sigma-Aldrich Corp., St. Louis, MO, USA) containing 10% fetal bovine serum (Invitrogen^{TM}, Carlsbad, CA, USA). HT-29 cells were grown in Roswell Park Memorial Institute (RPMI)-1640 medium (Sigma-Aldrich Corp.) containing 10% heated inactivated serum. Both cell lines were maintained in humidified air with 5% CO_2 at 37°C. For treated media, DMEM without bicarbonate (Sigma-Aldrich Corp.) was supplemented with 25mM 2-[4-(2-Hydroxyethyl)-1-piperazinyl] ethanesulfonic acid (HEPES; Dojindo Laboratories, Kumamoto, Japan). Medium was then adjusted to pH 7.5 and pH 6.5 for control and low pH medium, respectively, and then media were supplemented with 10% fetal bovine serum, which did not affect the medium pH.

Drug treatment

$2x10^5$ HeLa cells were seeded on 3.5 cm diameter dish and incubated at the growing condition for 24 hours. Then cells were treated with pre-warm control pH (pH 7.3) or low pH (pH 6.3) medium containing NO-RS-082 (ONO) (Biomol/Enzo Life Sciences, Inc. Farmingdale, NY, USA), bromoenol lactone (BEL) (Biomol), arachidonyl trifluoromethyl ketone (AACOCF3) (Sigma-Aldrich Corp.), methyl arachidonyl fluorophosphonate (MAFP) (Sigma-Aldrich Corp.) and cPLA2α inhibitor (Pyrrolidine derivative) (Calbiochem/ EMD Millipore, Billerica, MA, USA) for 30 minutes. The drug concentrations were described in Fig. 6.

Transfection and RNA interference

The following plasmids were used for protein expressions: Rab1 tagged with HA at N-terminus was transferred to pcDNA3.1 (Invitrogen™). β-1,3-N-acetylglucosaminyl transferase I tagged with GFP (GlcNAcT1-GFP) at C-terminus was transferred to pcDNA (Invitrogen™). β-1,4-galactosyl transferase fused pTagRFP (GalT-RFP) was purchased from Evrogen (Moscow, Russia). pTagRFP-T-N-SGG, which was kindly donated from Shibata laboratory (Nagoya Univ., Japan), was inserted with b1,3 N-acetylglucosaminyl transferase I (GlcNAcT1-RFP). 10^5 HeLa cells were seeded on coverslips in 3.5 cm diameter dish and incubated at the growing condition for 16 hours before transfection. Cells were transfected with plasmids using FuGENE®6 transfection reagent according to the manufacturer's protocol (Promega, Co., Madison, WI, USA). 100 µl of the total volume of medium containing DNA and FuGENE®6 transfection reagent was prepared per one dish. A pre-warm serum free medium was added with 3 µl of FuGENE®6 transfection reagent and 1 ng of plasmid DNA, then the transfection solution was incubated at room temperature for 15 minutes before transfection into cells.

For siRNA transfection, The following Stealth™ siRNA Duplex Oligonucleotides were used for transfection: YIPF1 (sense: 5'-AGAUCCUUU AAUUCUGUCAAAGACC-3', antisence: GGUCUUUGACAGAAUUAAAGGAUCU-3'), YIPF2 (sense: 5'-GUCAGCUG AUCGCUUCUGCUGGUGG-3', antisence: 5'-CCACCAGCAGAAGCGAUCAGCUGAC-3'). For YIPF6 knockdown, three siRNAs targeting difference YIPF6 sequence were mixed before transfection for reducing non-specific effects. The siRNA sequence of YIPF6 were: YIPF6#1 (sense: 5'-UUUAGAUCACGCAUGAUGGUAUUGC-3', antisence: 5'-GCAAU ACCAUCAUGCGUGAUCUAAA-3'), YIPF6#2 (sense: 5'-UAUACAGUAACCCAGCA CACAGAGG-3', antisence: 5'-CCUCUGUGUGCUGGGUUACUGUAUA-3'), YIPF6#3 (sense: 5'-AUAUCUGAAAGGCCUGCAAACAGGG-3', antisence: 5'-CCCUGUUUGCA

GGCCUUUCAGAUAU-3') (Invitrogen™). The control transfection was Silencer® Select Negative Control #1 siRNA (Ambion®). 10^5 HeLa cells were seeded on coverslips in 3.5 cm diameter dish and incubated at the growing condition for 16 hours before transfection. Cells were transfected with siRNAs using Lipofectamin™2000 according to the manufacturer's protocol (Invitrogen™). For each transfection sample, 5 µl of Lipofectamin™2000 was diluted in 250 µl Opti-Mem® I reduced serum medium, mixed gently and incubated for 5 minutes. The prepared reagent was added into 250 of Opti-Mem® I reduced serum medium containing 100 pmol of siRNA and incubated at room temperature for 20 minutes before transfection into cells, and then were incubated for 72 hours, changing medium every 24 hours.

SDS-Page and Western blot analysis

HeLa cells and HT-29 cells were extracted with lysis buffer (0.1M Tris-HCl (pH6.7), 4% SDS). Equal amount of proteins, 10 µg of lysed cell was loaded per well, were separated on 12% SDS-polyacrylamine gels. The electrophoresis was performed at 20mA, 500V, and then discontinuous gel electrophoresis was carried out. Proteins were transferred onto 0.45 µm pore size polyvinylidene fluoride (PVDF) (Immubilon®-P) at 100mA, 300V for 30 minutes using modified western blotting with Amersham ECL kit system. The PVDF membranes were blocked with 5% non-fat dry milk in 0.2% Tween-20 in PBS (-) (Wash buffer) and were then further incubated with primary antibodies, affinity purified polyclonal rabbit anti-YIPF1, anti-YIPF2 and anti-YIPF6 antibodies, which were produce by Nakamura laboratory (KSU, Japan). The PVDF membranes were washed with wash buffer for 1 hour, changing wash buffer every 15 minutes. The second antibodies incubation, the PVDF membrane were labeled with horseradish peroxidase (HRP)-conjugated rabbit anti-IgG antibody (Tago Immunologicals, Burlingame, CA) for 1 hour and again washed with wash

buffer for 1 hour, changing wash buffer every 15 minutes. Finally, the reactions were developed by Immubilon™ Western (Millipore®).

Immunofluorescence staining

The following antibodies were used for indirect immunofluorescence staining: for first antibodies, rabbit anti-human GM130 and rabbit anti-giantin (kindly donated by Dr. Misumi, Fukuoka Univ., Japan), mouse anti-GM130 monoclonal (BD Transduction Laboratories, Franklin Lakes, NJ, USA) and sheep anti-TGN46 (Serotec, Raleigh, NC). For secondary antibodies, Ax488 conjugated anti-rabbit (Molecular Probes Inc., Eugene, OR, USA), Ax488 conjugated anti-sheep, CY3 conjugated anti-mouse IgG, CY3 conjugated anti-sheep IgG, CY5 conjugated anti-mouse IgG and CY5 conjugated anti-rabbit IgG were used for the experiments (Jackson ImmunoReseach Labs. Inc., West Grove, PA, USA). High-affinity F-actin probe conjugated to the green fluorescent dye, fluorescein (FITC-phalloidin), was purchased from Invitrogen™.

HeLa cell grown on coverslips were fixed with 4% paraformaldehyde in 0.1M sodium phosphate buffer (PFA-PB) (pH7.4) for 20 minutes and washed with phosphate-buffered saline without Ca^{2+} and Mg^{2+} (PBS (-)) (Dulbecco and Vogt, 1954). 0.1% Triton X-100 in PBS was used for permeabilizing cells for 4 minutes and cells were washed with 0.2% (w/v) fish skin gelatin (Sigma-Aldrich Corp.) in PBS (-) (gelatin-PBS (-)). Then cells were incubated with gelatin-PBS (-) containing primary antibodies for 1 hour, washed three-times with PBS (-). The cells were incubated with secondary antibodies in gelatin-PBS (-) for 1 hour and again washed with PBS (-). Then cells were fixed with 4% paraformaldehyde for 20 minutes. For affinity purified polyclonal rabbit anti-YIPF1, anti-YIPF2 and anti-YIPF6 antibodies, 0.1% saponin was used for permeabilization by the incubation of 0.1% saponin in gelatin-PBS (-) containing primary or secondary antibodies. Finally, cells were mounted onto

slide with Vectachield solution (fluorophore protector) (Vector Labs. Inc., Burlingame, CA) or ProLong® Gold antifade reagent with DAPI (Invitrogen™).

Anterograde protein transport assay

VSV-G (tsO45)-EGFP fusion protein was excised from pcDNA3-VSVG-EGFP. Using an Adenovirus Expression Vector Kit VSV-G (tsO45)-EGFP fusion protein was inserted into cosmid pAxCAwt. Multiplicity of infection (MOI) was 500 for the VSV-G (tsO45)-EGFP expressing virus (Presley *et al*., 1997 and Yoshida *et al*., 2004). $2x10^5$ HeLa cells were seeded on coverslips in 3.5 cm diameter dish for 24 hours, and then cells were infected with a recombinant adenovirus expressing VSV-G (tsO45)-GFP and incubated for 24 hours at 39°C. Then the medium was replaced with pre-warm control or low pH medium and incubated cells at 39°C for 1 hour, and cells were further incubated with pre-warm control or low pH medium containing 100 µg/ml cycloheximide (Sigma-Aldrich Corp.) at 32.5 °C for the indicated time.

Electron microscopy

$2x10^5$ HeLa cells were spread on a Cell Desk™ (LF1, low fluorescence type, MS-92132 Sumitomo Bakelight), 24 hours later, were treated with pre-warm control (pH 7.3) or low pH (pH 6.3) medium for 30 minutes. The following procedure was carried out at room temperature. The cells were fixed with 2.5 glutardehyde in 0.1M cocadylate buffer (pH 7.3) for 2 hours, washed three-times and leaved in PBS (-) for 2 hours. The cells were washed three-times with 0.2M cocadylate buffer and treated with 1% osmium tetroxide in 0.1M sodium cacodylate buffer (pH7.3) for 1 hour. Then cells were washed three-times with distilled water and dehydrated by 30%, 50%, 70%, 90%, 95%, 100% and 100% of ethanol for 10, 10, 60, 10, 10, 10 and 10 minutes, respectively. The cells were further incubated in 50%

resin in 100% ethanol for 30 minutes, and then in were embedded two-times with Quetol 812 resin (Nisshin EM, Tokyo, Japan) for 1 hour. Cell Desks™ were cut into two pieces and placed on a silicone block filled with resin and bake at 60°C for 48 hours. Then ultra-thin sections were prepared and stained with 2% uranyl acetate for 60 minutes, and washed by dripping four-times in distilled water. The cells were further incubated in lead acetate 1 minute and again dripped four-times in distilled water. Sections were observed using a JEM-1210 electron microscope (Jeol Ltd., Tokyo, Japan). Immunoelectron microscopy using the gold enhancement method was also performed, as described previously

Periodic acid-Schiff (PAS) staining

$2x10^5$ HT-29 cells were seeded on coverslips in 3.5 cm diameter dish and transfected with siRNA as described in siRNA transfection method, then cells were stained with Periodic Acid Schiff (PAS) reagent according to the manufacturer's protocol (Sigma-Aldrich Corp.). The protocol was slight modification, briefly, cells were fixed with formalin-ethanol fixative solution (4% formaldehyde in 95% ethanol) and gently washed three-times with tap water. Periodic Acid solution was used for coverslip immersion, 5 minutes, and then cells were washed five-times with distilled water. Cells were immersed in Schiff's reagent for 15 minutes and washed ten-times with tap water. Coverslips were mounted with glycerol and observed by light microscope.

The in intensity of PAS staining was measured using imageJ. The areas of cell clusters were selected by free hand mode. Non-cell areas were selected for background. The intensity of all selection areas was calculated by the gray values of all the pixels in the selection divided by the number of pixels. Average intensity of cell cluster was subtracted with average intensity of background and the ratio to control group was calculated. Averages of three experiments were done.

Quantitative analysis of the Golgi structure

The following numbers of cells were counted for quantifying the percentage of cells with protected Golgi: 45, 39, 40, 42, 47 and 43 cells for 0, 67, 130, 270, 540 and 800 μM of ONO, respectively. 45, 48, 40, 47, 42 and 46 cells for 0, 16, 32, 80, 160 and 320 μM of BEL, respectively. For the analysis of the protective effect of PLA_2s against the low pH induced Golgi disassembly, the cells showing ribbon-like structure of the Golgi apparatus were identified as shown in Fig. 7A.

The following numbers of cells in three independent experiments were counted for quantifying the percentage of cell with intact Golgi: In control pH, 64, 61 and 83 cells for Control. 48, 59 and 69 cells for YIPF1 knockdown. 56, 64 and 84 cells for YIPF2 knockdown. 57, 72 and 94 cells for YIPF6 knockdown. 52, 64 and 74 cells for combination of YIPF1 and YIPF2 knockdown. In 15 minutes low pH treatment, 53, 53 and 79 cells for Control. 52, 67 and 76 cells for YIPF1 knockdown. 55, 56 and 72 cells for YIPF2 knockdown. 64, 67 and 79 cells for YIPF6 knockdown. 53, 58 and 73 cells for combination of YIPF1 and YIPF2 knockdown. In 30 minutes low pH treatment, 47, 54 and 76 cells for Control. 43, 63 and 73 cells for YIPF1 knockdown. 54, 64 and 72, cells for YIPF2 knockdown. 62, 70 and 83 cells for YIPF6 knockdown. 55, 63 and 79 cells for combination of YIPF1 and YIPF2 knockdown. For the analysis of the effect of YIPF1, YIPF2 and YIPF6 knockdown in low pH induced Golgi disassembly, the Golgi apparatus of HeLa cells, which were knocked down with YIPF1, YIPF2, YIPF6 or combination of YIPF1 and YIPF2 siRNA and treated with a low pH medium for 0, 15 and 30 minutes, were observed. The Golgi structure was characterized to intact and fragmented Golgi as shown in Fig. 15A. The number of cells with intact Golgi was counted and the ratio to the total cell number was calculated. Average of three experiments was done.

Acknowledgements

Firstly, I would like to gratefully and sincerely thank my advisor Professor Nobuhiro Nakamura (Department of Molecular Biosciences, Faculty of life science, Kyoto Sankyo University) for continuous support of my Ph. D study, understanding and patience. His guidance helped me to produce the entire this work and write this thesis. I would like to thank my thesis committee: Professor Kazuhiro Nagata (Department of Molecular Biosciences, Faculty of life science, Kyoto Sankyo University) and Associate Professor Kouki Kawane (Department of Molecular Biosciences, Faculty of life science, Kyoto Sankyo University), for their encouragement, insightful comments, and suggestion. I would like to gratefully thank Professor Keiko Kato (Department of Animal Medical Sciences, Faculty of life science, Kyoto Sankyo University) for her necessary guidance of PAS staining. I am also very thankful to Professor Akira Kurosaka (Department of Molecular Biosciences, Faculty of life science, Kyoto Sankyo University) for his advices that helped me to improve my work. I would like to thank Dr. Ryuichi Ishida, Shiho Osako and all members of Nakamura Laboratory for the discussion and all their supports that helped to perform my research.

Finally, I would like to thank my family for supporting me spiritually throughout staying abroad, learning in research field and writing this thesis.

References

Appenzeller-Herzog C and Hauri HP (2006) The ER-Golgi intermediate compartment (ERGIC): in search of its identity and function. J. Cell Sci.119. 2173–2183, http://dx.doi.org/10.1242/ jcs.03019.

Barrowman, J., Wang, W., Zhang, Y. and Ferro-Novick, S. (2003). The Yip1p -Yif1p complex is required for the fusion competence of endoplasmic reticulum-derived vesicles, J. Biol. Chem. 278, 19878–19884

Bechler M.E., Doody AM, Racoosin E, Lin L, Lee KH, Brown WJ (2010). The phospholipase complex PAFAH Ib regulates the functional organization of the Golgi complex. J Cell Biol. 190, 45–53.

Bechler, M.E., De Figueiredo, P., Brown, W. J. (2012). A PLA1-2 punch regulates the Golgi complex, Trends Cell Biol. 22, 116–124, http://dx.doi.org/10.1016/j.tcb.2011.10.003.

Bechler, M.E., Doody, A.M., Ha, K.D., Judson, B.L. (2011). Chen, I.; Brown, W.J. The phospholipase A2 enzyme complex PAFAH Ib mediates endosomal membrane tubule formation and trafficking. Mol. Biol. Cell. 22, 2348–2359, http://dx.doi.org/10.1091/mbc.E09-12-1064. 21593204.

Beck, R., Rawet, M., Wieland, Cassel, F.T., D.. (2009). The COPI system: Molecular mechanisms and function. FEBS Lett. 583, 2701–2709, http://dx.doi.org/10.1016/j.febslet.2009.07.032.

Brandl, K., Tomisato, W., Lia, X., Neppl, C., Pirie, E., Falk, W., Xia, Y., Moresco, Eva Marie Y., Baccala, R., Theofilopoulos, A. N., Schnabl, B. and Beutler, B. (2012). Yip1 domain family, member 6 (Yipf6) mutation induces spontaneous intestinal inflammation in mice. Proc. Natl. Acad. Sci. USA. 109(31): 12650–12655, http://dx.doi.org/10.1073/pnas.1210366109.

Brockhausen, I. (1999). Pathways of O-glycan biosynthesis in cancer cells. *Biochim Biophys Acta*. 1473, 67–95.

Brown, A.K., Hunt, S.D., and Stephens, D.J. (2014) Opposing microtubule motors control motility, morphology, and cargo segregation during ER-to-Golgi transport. Biology Open 3, 307-313, http://dx.doi.org/10.1242/bio.20147633.

Bucci, C., Lutcke, A., Steele-Mortimer, O., Olkkonen, V. M., Dupree, P., Chiariello, M., Bruni, C. B., Simons, K. and Zerial, M. (1995). Co-operative regulation of endocytosis by three Rab5 isoforms. FEBS Lett. 366, 65-71.

Bucci, C., Thomsen, P., Nicoziani, P., McCarthy, J. and van Deurs, B. (2000). Rab7: a key to lysosome biogenesis. Mol. Biol. Cell. 11, 467-480.

Cai, H., Reinisch, K., Ferro-Novick, S. (2007a). Coats, tethers, Rabs, and SNAREs work together to mediate the intracellular destination of a transport vesicle. Dev Cell, http://dx.doi.org/10.1016/j.devcel.2007.04.005.

Cosson, P., de Curtis, I., Pouyssegur, J., Griffiths, G. and Davoust, J. (1989). Low cytoplasmic pH inhibits endocytosis and transport from the trans-Golgi network to the cell surface. J. Cell Biol. 1083, 77–387.

Dippold, H.C., Ng, M.M., Farber-Katz, S.E., Lee, S.-K., Kerr, M.L., Peterman, M.C., Sim, R., Wiharto, P.A., Galbraith, K.A., Madhavarapu, S., Fuchs, G.J., Meerloo, T., Farquhar, M.G., Zhou, H., Field, S.J. (2009). GOLPH3 bridges phosphatidylinositol-4- phosphate and actomyosin to stretch and shape the Golgi to promote budding. Cell. 139, 337–351.

Dykstra KM, Pokusa JE, Suhan J, Lee TH (2010) Yip1A structures the mammalian endoplasmic reticulum. Mol Biol Cell 21: 1556–1568.

Glick BS, Luini A (2011) Models for Golgi traffic: a critical assessment. Cold Spring Harb. Perspect. Biol. 3, a005215, http://dx.doi.org/10.1101/cshperspect.a005215.

Glunde, K., Guggino, S. E., Solaiyappan, M., Pathak, A. P., Ichikawa, Y., & Bhujwalla, Z. M. (2003). Extracellular Acidification Alters Lysosomal Trafficking in Human Breast Cancer Cells. Neoplasia (New York, N.Y.). 5(6), 533–545.

Haas, A. K., Yoshimura, S., Stephens, D.J., Preisinger, C., Fuchs, E., Barr, F.A. (2007). Analysis of GTPase-activating proteins: Rab1 and Rab43 are key Rabs required to maintain a functional Golgi complex in human cells. J. Cell Sci. 120, 2997-3010

Heidtman , M., Chen, C.Z., Collins, R.N. and Barlowe, C. (2003). A role for Yip1p in COPII vesicle biogenesis, J. Cell Biol, 163 57–69.

Heidtman , M., Chen, C.Z., Collins, R.N. and Barlowe, (2005). Yos1p Is a Novel Subunit of the Yip1p–Yif1p Complex and Is Required for Transport between the Endoplasmic Reticulum and the Golgi Complex, Molecular Biology of the Cell Vol. 16, 1673–1683, http://dx.doi.org 10.1091/mbc.E04-10-0873.

Heuser, J. (1989). Changes in lysosome shape and distribution correlated with changes in cytoplasmic pH. J. Cell Biol. 108,855–864.

Hicks, S.W., Machamer, C.E. (2005). Golgi structure in stress sensing and apoptosis. Biochim Biophys Acta. 1744, 406-414, doi:10.1016/j.bbamcr.2005.03.002

Ho, W. C., Allan, V. J., van Meer, G., Berger, E. G. and Kreis, T. E. (1898). Reclustering of scattered Golgi elements occurs along microtubules. Eur J Cell Biol. 48(2), 250-63.

Jedd,G., Mulholland,J. and Segev,N. (1997) Two new Ypt GTPases are required for exit from the yeast trans-Golgi compartment. J. Cell Biol., 137, 563–580.

Jedd,G., Richardson,C., Litt,R. and Segev,N. (1995) The Ypt1 GTPase is essential for the first two steps of the yeast secretory pathway. J. Cell Biol., 131, 583–590.

Joshi G, Chi Y, Huang Z, Wang Y (2014) Aβ-induced Golgi fragmentation in Alzheimer's disease enhances Aβ production. Proc. Natl. Acad. Sci. USA. 111(13), E1230-E1239.

Kano, F., Yamauchi, S., Yoshida, Y., Watanabe-Takahashi, M., Nishikawa, K., Nakamura, N., Murata M. (2009). Yip1A regulates the COPI-independent retrograde transport from the Golgi complex to the ER. J. Cell Sci. 122, 2218–2227, http://dx.doi.org/10.1242/jcs.043414.

Keller, P. and Simons, K. (1997). Post-Golgi biosynthetic trafficking. J Cell Sci.*110*, 3001–3009.

Kienzle, C. and von Blume, J. (2014) Secretory cargo sorting at the trans-Golgi network. Trends Cell Biol. 24, 584-593.

Klausner, R. D., Donaldson, J. G. and Lippincott-Schwartz, J. (1992). Brefeldin A: Insights into the Control of Membrane Traffic and Organelle Structure. J. Cell Biol. 116(5), 1071-1080.

Ladinsky, M.S., Kremer, J.R., Furcinitti, P.S., Mcintosh, J.R., Howell, K.E. (2002). Structure of the Golgi and distribution of reporter molecules at 20 degrees C reveals the complexity of the exit compartments, Mol. Biol. Cell. 13, 2810– 2825.

Lippincott-Schwartz, J., Yuan, L., Bonifacino, J. and Klausner, R. (1989). Rapid redistribution of Golgi proteins into the ER in cells treated with Brefeldin A: evidence for membrane cycling from Golgi to ER. Cell. 56, 801-813.

Liu, S., & Storrie, B. (2012). Are Rab Proteins the Link Between Golgi Organization and Membrane Trafficking? Cellular and Molecular Life Sciences : CMLS. 69(24), 4093–4106, http://doi.org/10.1007/s00018-012-1021-6.

Liu, S., Hunt, L., Storrie, B., (2013). Rab41 is a novel regulator of Golgi apparatus organization that is needed for ER-to-Golgi trafficking and cell growth. PLoS One. 8(8), e71886, http://doi.org/ 10.1371/journal.pone.0071886.

Lowe, M., Rabouille, C., Nakamura, N., Watson, R., Jackman, M., Jamsa, E., Rahman, D., Pappin, D.J., and Warren, G. (1998a). Cdc2 kinase directly phosphorylates the *cis*-

Golgi matrix protein GM130 and is required for Golgi fragmentation in mitosis. Cell. 94, 783–793, http://dx.doi.org/10.1016/S0092-8674(00)81737-7.

Lupashin, V., Sztul, E. (2005). Golgi tethering factors, *Biochim Biophys Acta*.1744,325 – 339., doi:10.1016/j.bbamcr.2005.03.013

Martinez-Alonso, E. and Tomas, M. (2013). Golgi tubules: their structure, formation and role in intra-Golgi transport, Histochem. Cell Biol. 140(3), 327–339, 2013.

Matern, H., Yang, X., Andrulis, E., Sternglanz, R., Trepte, H. H., and Gallwitz, D. (2000). A novel Golgi membrane protein is part of a GTPase-binding protein complex involved in vesicle targeting. EMBO J. 19, 4485–4492.

Mollenhauer, H.H. and Morré, D.J., (1993). The tubular network of the Golgi apparatus. Histochem Cell Biol, 109(5-6),533-43.

Nakamura, N., M. Lowe, T. P. Levine, C. Rabouille and G. Warren. (1997). The vesicle docking protein p115 binds GM130, a *cis*-Golgi matrix protein, in a mitotically regulated manner. Cell. 89, 445–455.

Niu, T.K., Pfeifer, A.C., Lippincott-Schwartz, J., Jackson, C.L., (2005). Dynamics of GBF1, a brefeldin A-sensitive Arf1 exchange factor at the Golgi, Mol Biol Cell. 16, 1213–1222, http://dx.doi.org/10.1091/mbc.E04-07-0599.

Orci, L., Ravazzola, M., Volchuk, A., Engel, T., Gmachl, M., Amherdt, M., Perrelet, A., Sollner, TH., Rothman, J.E. (2000b) Anterograde flow of cargo across the Golgi stack potentially mediated via bidirectional 'percolating' COPI vesicles. Proc. Natl. Acad. Sci. USA. 97, 10400–10405.

Parton, R.G., Dotti, C.G., Bacallao, R., Kurtz, I., Simons, K., Prydz, K. (1991). pH-induced microtubule-dependent redistribution of late endosomes in neuronal and epithelial cells. J Cell Biol. 113(2),261–274.

Presley, J.F., Cole, N.B., Schroer, T.A., Hirschberg, K., Zaal, K.J., Lippincott-Schwartz, J. (1997). ER-to-Golgi transport visualized in living cells. Nature 389, 81–85.

Rambourg, A., and Clermont, Y. (1990). Three-dimensional electron microscopy: structure of the Golgi apparatus. Eur. J. Cell Biol., 51, 189-200.

Salminen, A. and Novick, P. J. (1987). A ras-like protein is required for a post-Golgi event in yeast secretion. Cell. 49, 527-538.

Schmitt, H. D., Wagner, P., Pfaff, E. and Gallwitz, D. (1986). The ras-related YPT1 gene product in yeast: a GTP-binding protein that might be involved in microtubule organization. Cell. 47, 401-412.

Schwartz, S.L., Cao, C., Pylypenko, O., Rak, A., Wandinger-Ness, A. (2007). Rab GTPases at a glance, J. Cell Sci. 120, 3905–3910.

Schwarz, F. and Aebi, M. (2011). Mechanisms and principles of N-linked protein glycosylation. Current Opinion in Structural Biology. 21:576–582, http://dx.doi.org/10.1016/j.sbi.2011.08.005.

Shakoori, A., Fujii, G., Yoshimura , S., Kitamura , M., Nakayama, K., Ito, T., Ohno, H., Nakamura, N. (2003). Identification of a five-pass transmembrane protein family localizing in the Golgi apparatus and the ER, Biochem. Biophys. Res. Commun. 312, 850–857.

Shorter, J. and Warren, G. (2002). Golgi architecture and inheritance. Annu Rev Cell Dev Biol. 18:379–420, http://dx.doi.org/10.1146/annurev.cellbio.18.030602.133733.

Soonthornsit , J., Yamaguchi, Y., Tamura, D., Ishida, R., Nakakoji, Y., Osako, S., Yamamoto, A., Nakamura, N. (2014). Low cytoplasmic pH reduces ER-Golgi trafficking and induces disassembly of the Golgi apparatus, Exp Cell Res. 328, 325-39, http://dx.doi.org/10.1016/j.yexcr.2014.09.009.

Stanley, P. (2011). Golgi Glycosylation. *Cold Spring Harbor Perspectives in Biology*, *3*(4), a005199, http://dx.doi.org/10.1101/cshperspect.a005199.

Tang, D., & Wang, Y. (2013). Cell cycle regulation of Golgi membrane dynamics. *Trends Cell* Biol. 23(6), 296–304, http://dx.doi.org/10.1016/j.tcb.2013.01.008.

Tanimoto, K., Suzuki, K., Jokitalo, E., Sakai, N., Sakaguchi, T., Tamura, D., Fujii, G., Aoki, K., Takada, S., Ishida, R., Tanabe, M., Itoh, H., Yoneda, Y., Sohda, M., Misumi, Y., and Nakamura, N. (2011). The characterization of YIPF3 and YIPF4, *cis*-Golgi localizing Yip Domain family protein, *Cell* Struct. Funct. 36, 171–185.

Taylor, R. S., Jones, S. M., Dahl, R. H., Nordeen, M. H., and Howell, K. E. (1997). Characterization of the Golgi complex cleared of proteins in transit and examination of calcium uptake activities," Mol. Cell Biol. 8(10), 1911–1931.

Thayer, D. A., Jan, Y. N., and Jan, L. Y. (2013). Increased neuronal activity fragments the Golgi complex, Proc. Natl. Acad. Sci. USA. 110, 1482–1487, http://dx.doi.org/10.1073/pnas.1220978110.

Wagner, M., A.K. Rajasekaran, D.K. Hanzel, S. Mayor, and E. Rodriguez-Boulan. (1994). Brefeldin A causes structural and functional alterations of the trans-Golgi network of MDCK cells. J. Cell Sci. 107, 933-943.

Warren, G., Levine, T., & Misteli, T. (1995). Mitotic disassembly of the mammalian Golgi apparatus. *Trends Cell* Biol. 5, 413–416.

Wilson, B. S., Nuoffer, C., Meinkoth, J. L., McCaffery, M., Feramisco, J. R., Balch, W. E. (1994). Farquhar, M. G., A Rab1 mutant affecting guanine nucleotide exchange promotes disassembly of the Golgi apparatus. J Cell Biol. May;125(3), 557-71.

Xiao,H., Li,T.K., Yang,J.M. and Liu,L.F. (2003). Acidic pH induces topoisomerase II‐mediated DNA damage. Proc. Natl Acad. Sci. USA, 100, 5205–5210.

Xu, L., Fukumura, D., Jain, R.K. (2002). Acidic extracellular pH induces vascular endothelial growth factor (VEGF) in human glioblastoma cells via ERK1/2 MAPK signaling pathway: mechanism of low pH-induced VEGF. J Biol Chem. 277, 11368–11374, http://dx.doi.org/10.1074/jbc.M108347200.

Yang, X., Matern ,H.T., Gallwitz , D. (1998). Specific binding to a novel and essential Golgi membrane protein (Yip1p) functionally links the transport GTPases Ypt1p and Ypt31p, EMBO J. 17, 4954–4963.

Yoshida, T., Kamiya, T., Imanaka-Yoshida, K., Sakakura, T. (1999). Low cytoplasmic pH causes fragmentation and dispersal of the Golgi apparatus in human hepatoma cells, Int. J. Exp. Pathol. 8051–57.

Yoshida, Y., Suzukia Kurum.i, Yamamoto A., Sakaia N., Bando, M., Tanimoto, Kouji., Yamaguchi Y., Sakaguchi, T., Akhter, H., Fujii, G., Yoshimur, S., Ogata, S., Sohda, Miwa., Misum, Y., Nakamura N. (2008). YIPF5 and YIF1A recycle between the ER and the Golgi apparatus and are involved in the maintenance of the Golgi structure, Exp Cell Res. 314, 3427–3443, http://dx.doi.org/10.1016/j.yexcr.2008.07.023.

Yoshimura, S., Yamamoto, A., Misumi, Y., Sohda, M., Barr, F.A., Fujii, G., Shakoori, A., Ohno, H., Mihara, K., Nakamura, N. (2004). Dynamics of Golgi matrix proteins after the blockage of ER to Golgi transport, J.Biochem. 135, 201–216, http://dx.doi.org/10.1093/jb/mvh024.

Figure Legends

Figure 1. The reversible disassembly of Golgi apparatus in low pH medium

A, HeLa cells were incubated with a low pH medium (pH6.3) for 0, 15, 30 and 60 minutes, and then cells were further incubated (R) with a control pH medium (pH7.3) for 15, 30, 60 and 120 minutes. B, HEK293 cells were incubated with a low pH medium for 0, 30 and 60 minutes, and then cells were further incubated (R) with a control pH medium for 15, 60 and 120 minutes. Cells were processed for immunofluorescence staining with anti-GM130 and anti-giantin antibodies. Projection pictures of confocal microscopy of Fig. 1A and epi-fluorescence images of Fig. 1B were shown. Arrow head indicated the tubule. Scale bar = 10 μm.

Figure 2. *Cis*-Golgi was significantly separated from *medial-/trans*-Golgi and TGN in low pH medium.

HeLa cells were transfected with GalT-RFP with/without GlcNAc-T1-GFP, and incubated with a low pH medium (pH6.3) for 15 or 30 minutes. The cells were then processed for immunofluorescence staining with anti-GM130 and anti-TGN antibodies. Projection pictures of confocal microscopy are shown. Arrow head indicated the tubule. Scale bar = 5 μm.

Figure 3. The disassembly of Golgi stack in low pH medium

HeLa cells were incubated with control pH or low pH medium for 30 minutes and then the cells were fixed and processed for electron microscopy. Arrowheads indicated the Golgi apparatus. Scale bar = 0.5 μm.

Figure 4. The transport of VSV-G (tsO45)-GFP was delayed in low pH condition.

VSV-G (tsO45)-GFP protein was allowed to express in HeLa cells and accumulate in the ER for 16 hours at 39.5˚C. The cells were then treated with a control pH medium (upper gallery) or a low pH medium for 1 hour (lower gallery) at 39.5˚C, and then incubated at 32˚C in the presence of cycloheximide. Cells were fixed and processed for immunofluorescence staining with anti-GM130 antibody. Epi-fluorescence images are shown. Scale bar = 10 μm.

Figure 5. Actin filament structure was not affected by the low pH treatment.

HeLa cells were incubated with control or low pH medium for 30 minutes. The cells were then fixed and processed for double immunofluorescence staining with anti-GM130 antibody and FITC-phalloidin. Epi-fluorescence images are shown. Scale bar = 10 μm.

Figure 6. ONO and BEL, PLA_2 inhibitors, prevented low pH-induced Golgi disassembly.

HeLa cells were incubated with a control or a low pH medium containing various concentrations of ONO, BEL, cPLA2α inhibitor, AACOCF3, or MAFP as indicated for 30 minutes. The cells were then fixed and processed for immunofluorescence staining with anti-GM130 antibodies. Epi-fluorescence images are shown. Scale bar = 10 μm.

Figure 7. Quantitation of the protective effect of ONO and BEL against the low pH induced Golgi disassembly.

The numbers of the cells showing protective effect of ONO and BEL under low pH condition in Fig. 6 were counted. A, The criteria of cell with protected or non-protected Golgi for counting. Scale bar = 10 μm. B, The relative percentage of cell with protected Golgi, which ratios to the non-treated group, is shown.

Figure 8. The overexpression of Rab1 suppressed low pH-induced Golgi disassembly and dispersal.

HeLa cells were transfected HA-Rab1and then incubated with control (pH 7.3) or low pH (6.3) medium for 30 minutes. The cell were fixed and processed for immunofluorescence staining with anti-HA and anti-GM130 antibodies. Epi-fluorescence images are shown. Scale bar = 10 μm.

Figure 9. The overexpression of Rab1 did not rescue the transport of VSV-G (tsO45)-GFP in low pH medium.

HeLa cells were transfected with HA-Rab1, and then VSV-G (tsO45)-GFP protein was allowed to express and accumulate in the ER for 16 hours at 39.5˚C. The cells were then treated with a control pH medium (upper gallery) or a low pH medium for 1 hour (lower gallery) at 39.5˚C and then incubated at 32˚C in the presence of cycloheximide. Cells were fixed and processed for immunofluorescence staining with anti-HA and anti-GM130 antibody. Epi-fluorescence images are shown. Scale bar = 10 μm.

Figure 10. The high temperature suppressed the function of Rab1.

The transfected HA-Rab1 cells were incubated at 32˚C, 37˚C and 39.5˚C for 1 hour, and then incubated with a control pH medium (upper gallery) or a low pH medium for 1 hour at the same temperatures for 30 minutes. The cells were then fixed and processed for immunofluorescence staining with anti-GM130 antibody. Epi-fluorescence images are shown. Scale bar = 10 μm.

Figure 11. YIPF1, YIPF2 and YIPF6 localized on *medial-*, *trans-* and TGN Golgi compartments.

HeLa cells were fixed and processed for double immunofluorescence staining with anti YIPFs protein and anti-Golgi marker proteins as described in Figure 2. Sliced pictures of confocal microscopy are shown. Scale bar = 5 µm

Figure 12. **Relocalization of YIPF1, YIPF2 and YIPF6 in the low pH medium**

HeLa cells were incubated with a low pH medium (pH 6.3) for 15 minutes, and then cells were fixed and processed for double immunofluorescence staining with anti YIPFs antibodies and anti-Golgi marker antibodies as described in Figure 2. Sliced pictures of confocal microscopy are shown. Scale bar = 5 µm

Figure 13. **Knockdown of YIPF1, YIPF2, and YIPF6**

HeLa cells were singly transfected with siRNAs for YIPF1, YIPF2, YIPF6 or doubly transfected with siRNAs for YIPF1 and YIPF2. After 72 hours, the cells were lysed and subjected to western blot analysis. A, Representative result of western blot analysis is shown. B, The amount of YIPF1, YIPF2 and YIPF6 were analyzed and the averages of the three independent experiments are shown. Bars indicate the standard deviation (SD).

Figure 14. The structure of the Golgi apparatus in YIPFs knockdown cells

HeLa cells were transfected with siRNAs as described in Fig. 13. After 72 hours, the cells were incubated with a low pH medium for 0, 15 and 30 minutes. Then the cells were fixed and processed for double immunofluorescence staining with anti-GM130, anti-giantin and anti-TGN46 antibody. Epi-fluorescence images are shown. Scale bar = 10 µm.

Figure 15. Quantitation of the protective effect for the low pH induced disassembly by the knockdown of YIPFs.

The numbers of the cell showing intact Golgi at 0, 15 and 30 minutes after the low pH treatment were counted. A, The criteria of intact and fragmented Golgi for counting. Scale bar = 10 μm. B, The relative percentage of intact Golgi, which ratios to the control group is shown. The averages of the three independent experiments are shown. Bars indicate SD.

Figure 16. The effect of YIPF1, YIPF2 and YIPF6 single and double knockdowns in glycoprotein production

A, HT-29 cells were transfected with siRNAs as described in Fig. 13. After 72 hours, the cells were lysed and analyzed by western blot analysis. A representative result of three independent experiments is shown. B, The result in A was quantified by image analysis as described in the Materials and Methods. C, The transfected cells were fixed after 72 hours and processed for PAS staining. Light microscopic images were shown. Scale bar = 100 μm. A representative result of three independent experiments is shown. D, The intensity of PAS staining was quantitated and relative levels to the control transfection were calculated as described in the Materials and Methods. The averages of the three independent experiments are shown. Bars indicate SD.

Figure 1

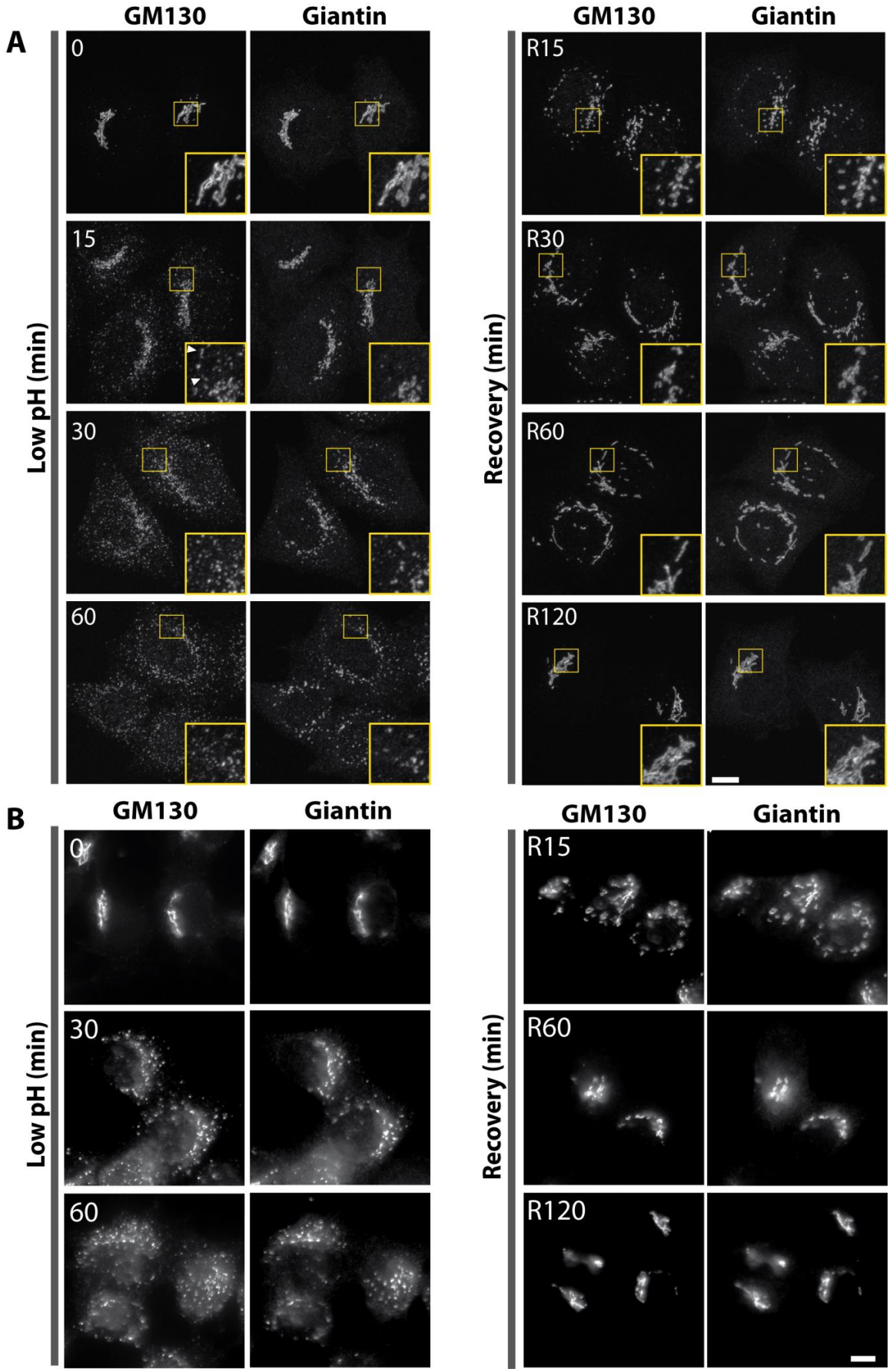
A
GM130
Giantin
Low pH (min)
0
15
30
60
Recovery (min)
R15
R30
R60
R120
B
GM130
Giantin
Low pH (min)
0
30
60
Recovery (min)
R15
R60
R120

Figure 2

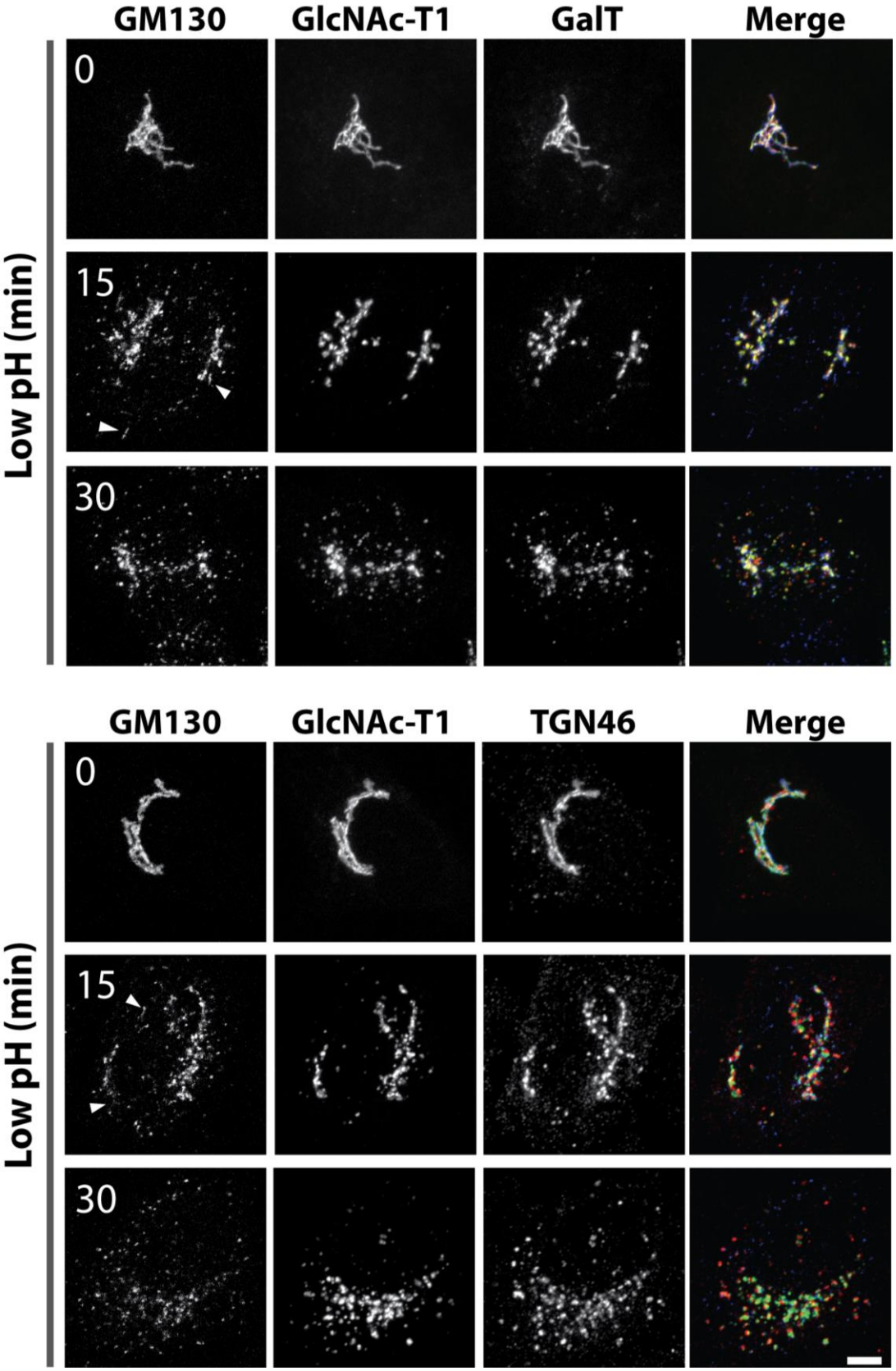
GM130
GlcNAc-T1
GalT
Merge
0
15
30
Low pH (min)
GM130
GlcNAc-T1
TGN46
Merge
0
15
30
Low pH (min)

Figure 3

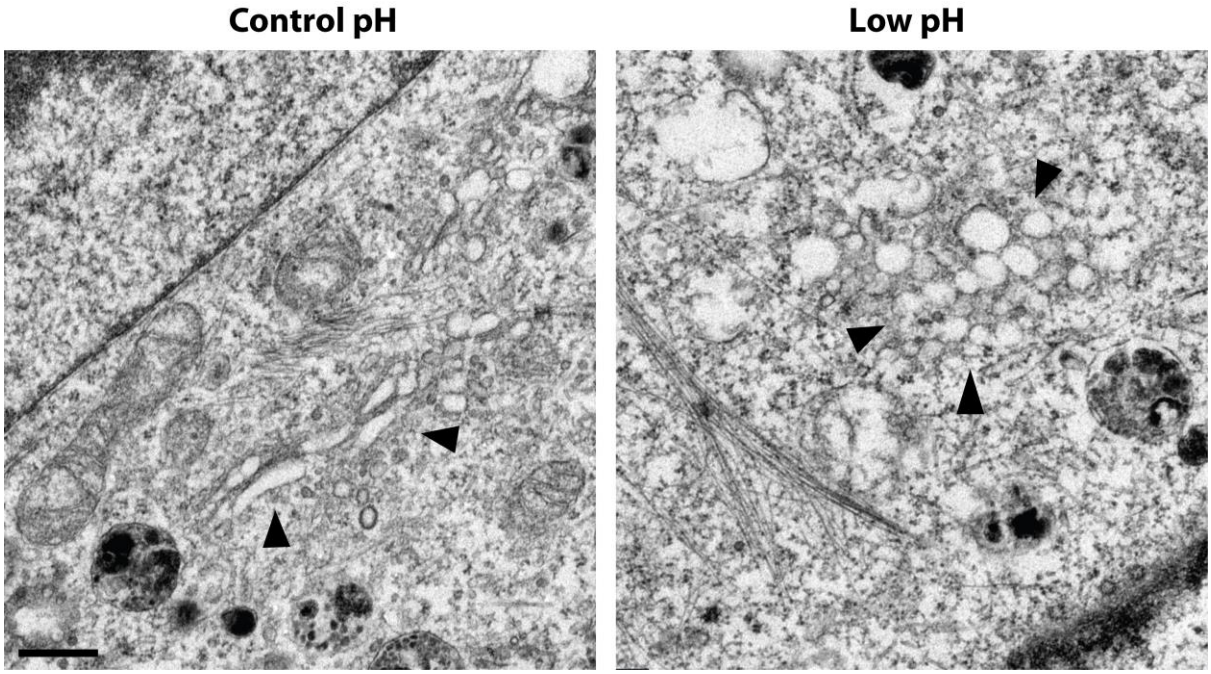

Figure 4

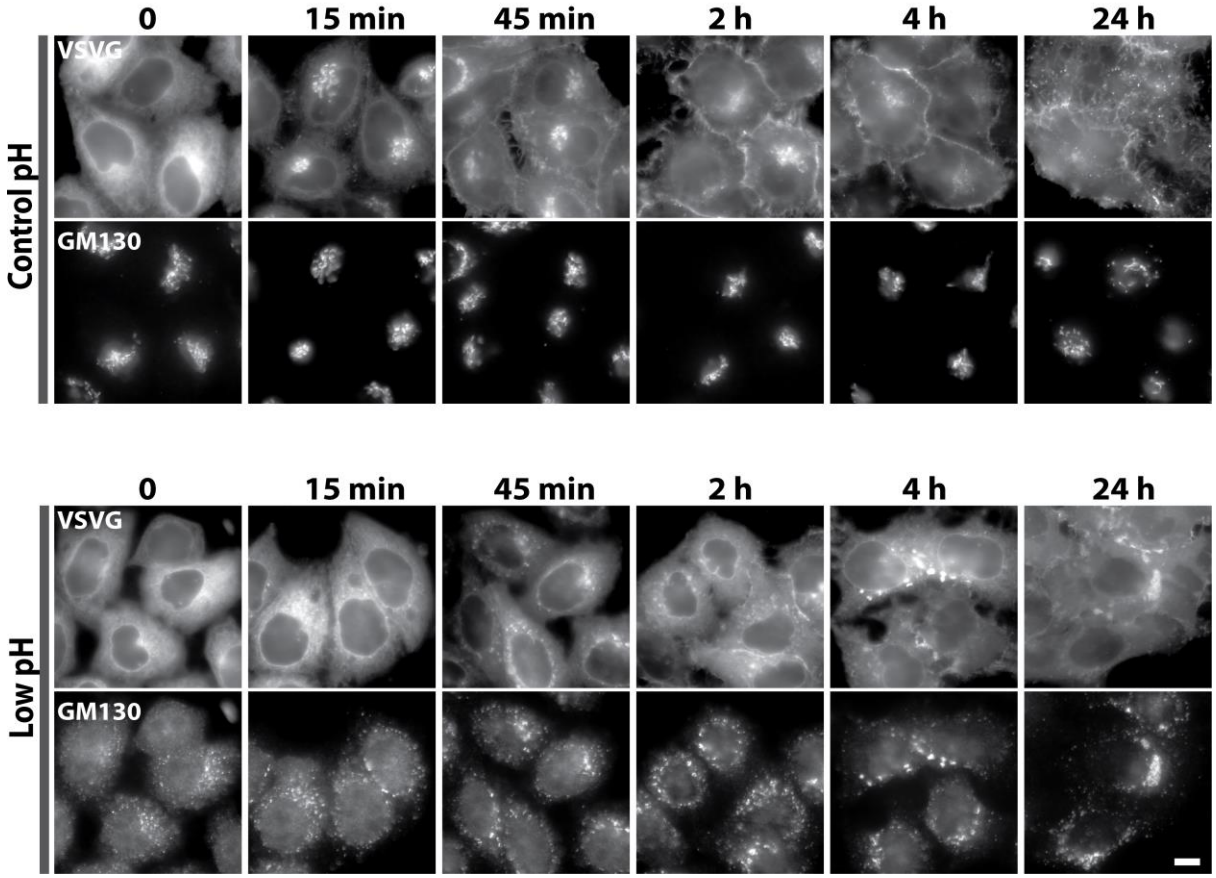
0
15 min
45 min
2 h
4 h
24 h
VSVG
GM130
Control pH
0
15 min
45 min
2 h
4 h
24 h
VSVG
GM130
Low pH

Figure 5

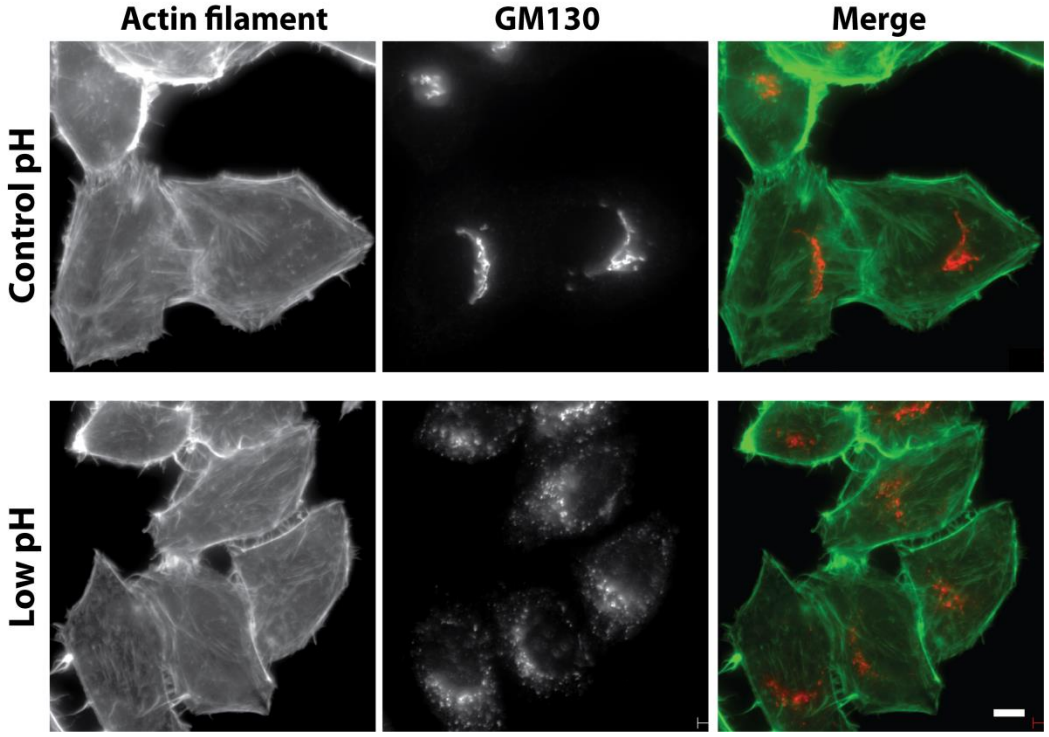

Figure 6

A

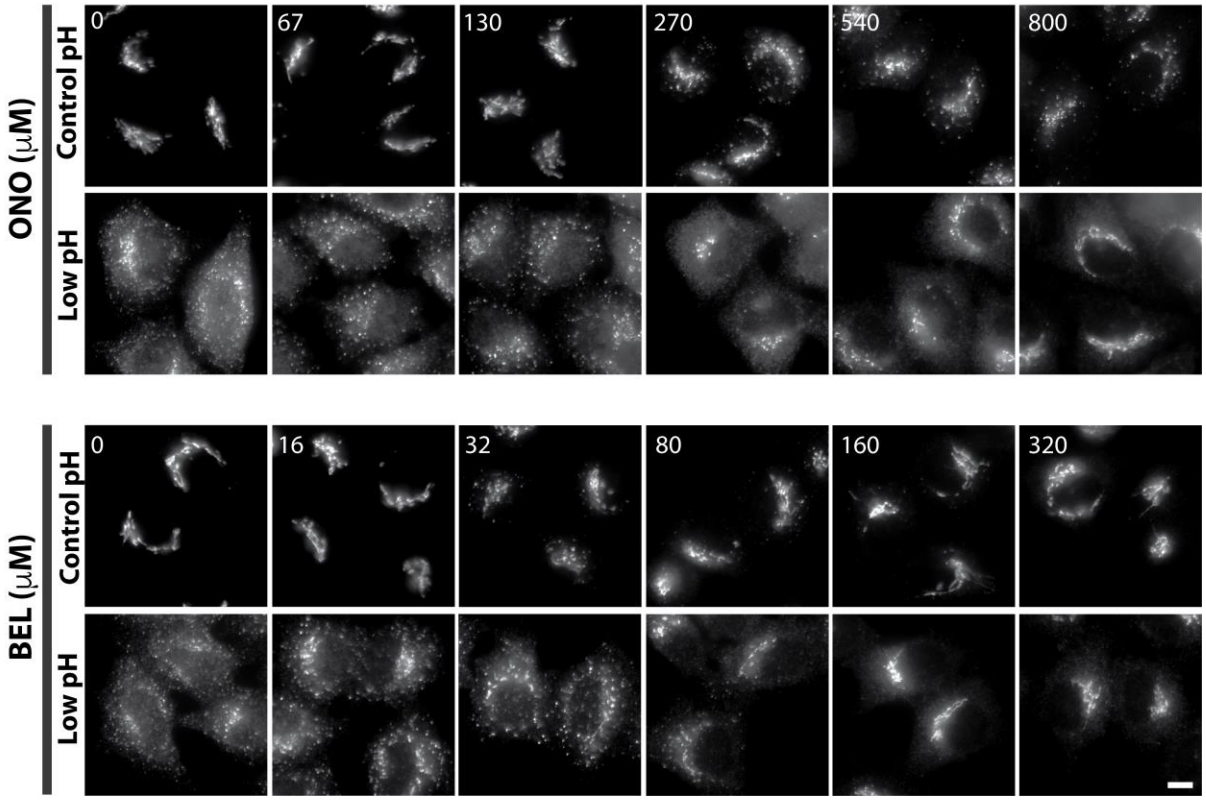
ONO (μM)
Control pH
Low pH
0
67
130
270
540
800
BEL (μM)
Control pH
Low pH
0
16
32
80
160
320

Figure 6

B

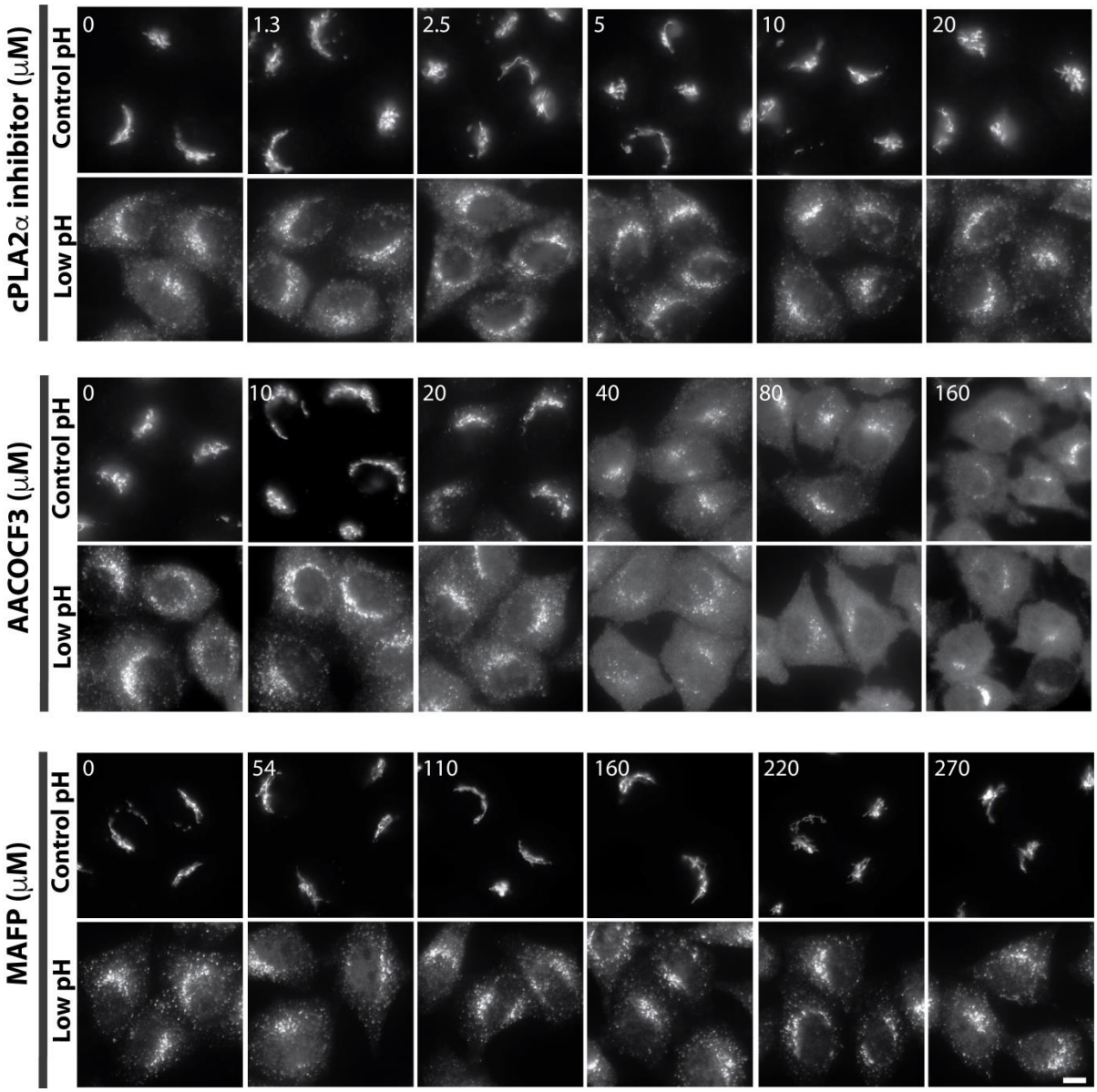
cPLA2α inhibitor (μM)
Control pH
Low pH
0
1.3
2.5
5
10
20
AACOCF3 (μM)
Control pH
Low pH
0
10
20
40
80
160
MAFP (μM)
Control pH
Low pH
0
54
110
160
220
270

Figure 7

A

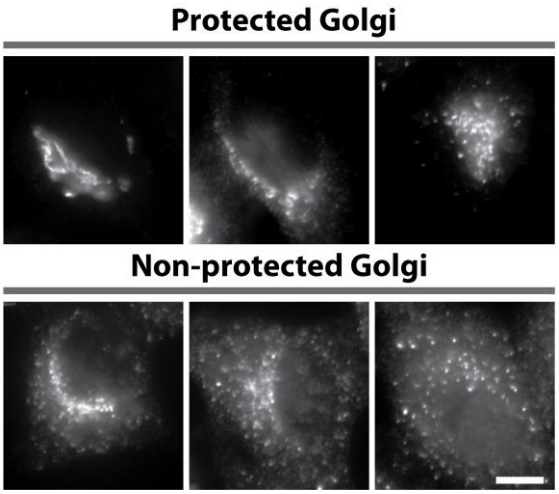
Protected Golgi
Non-protected Golgi

B

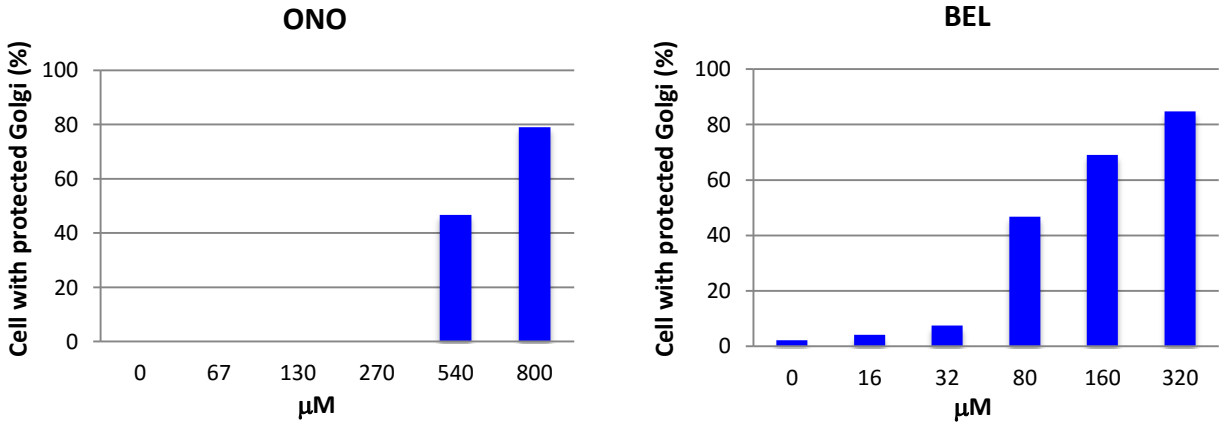
ONO
Cell with protected Golgi (%)
100
80
60
40
20
0
0
67
130
270
540
800
μM
BEL
Cell with protected Golgi (%)
100
80
60
40
20
0
0
16
32
80
160
320
μM

Figure 8

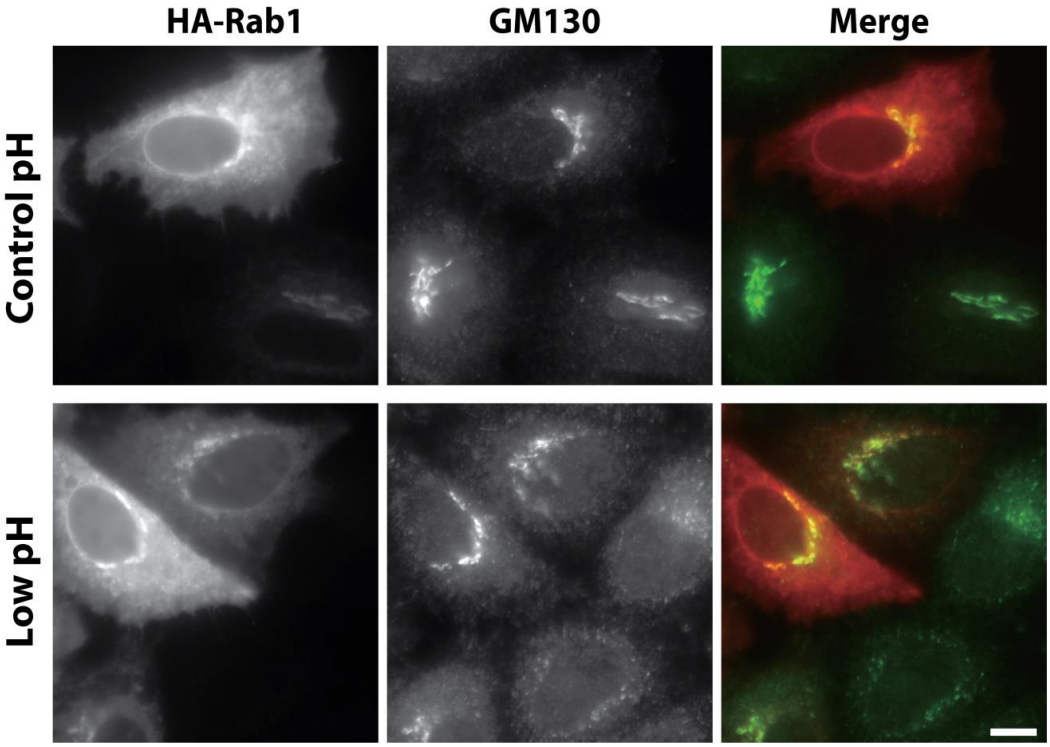

Figure 9

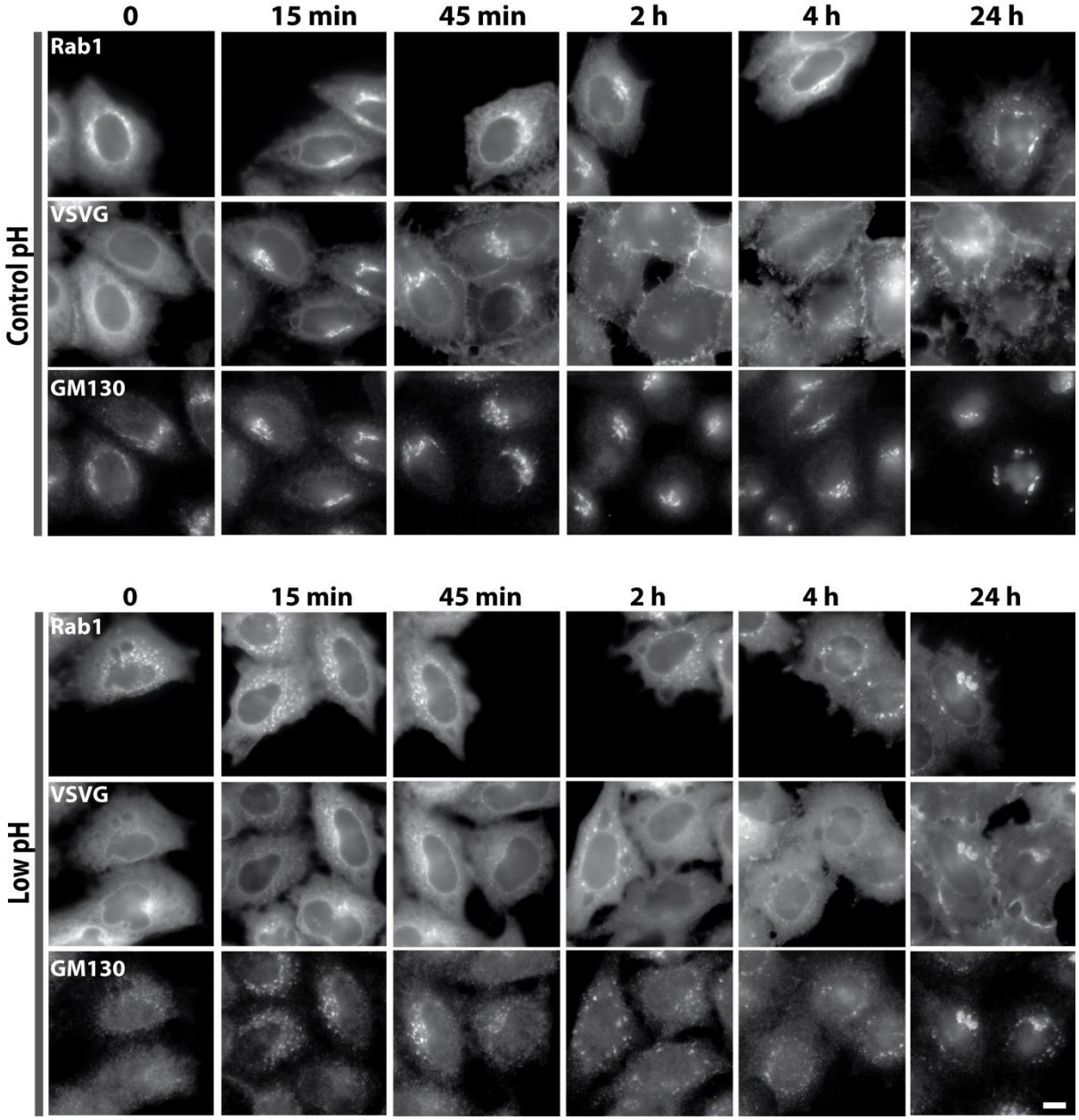
0
15 min
45 min
2 h
4 h
24 h
Rab1
VSVG
GM130
Control pH
0
15 min
45 min
2 h
4 h
24 h
Rab1
VSVG
GM130
Low pH

Figure 10

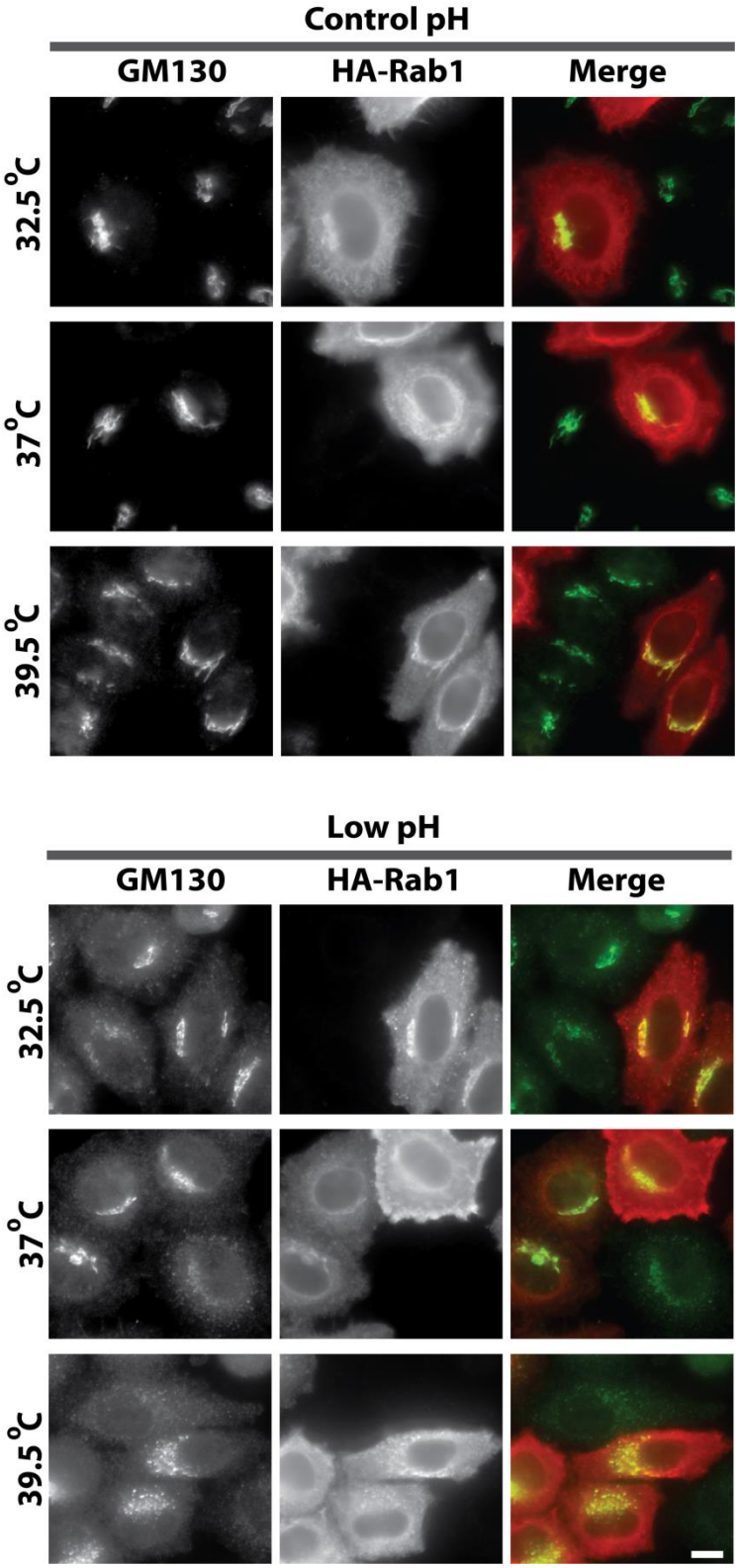
Control pH
GM130
HA-Rab1
Merge
32.5°C
37°C
39.5°C
Low pH
GM130
HA-Rab1
Merge
32.5°C
37°C
39.5°C

Figure 11

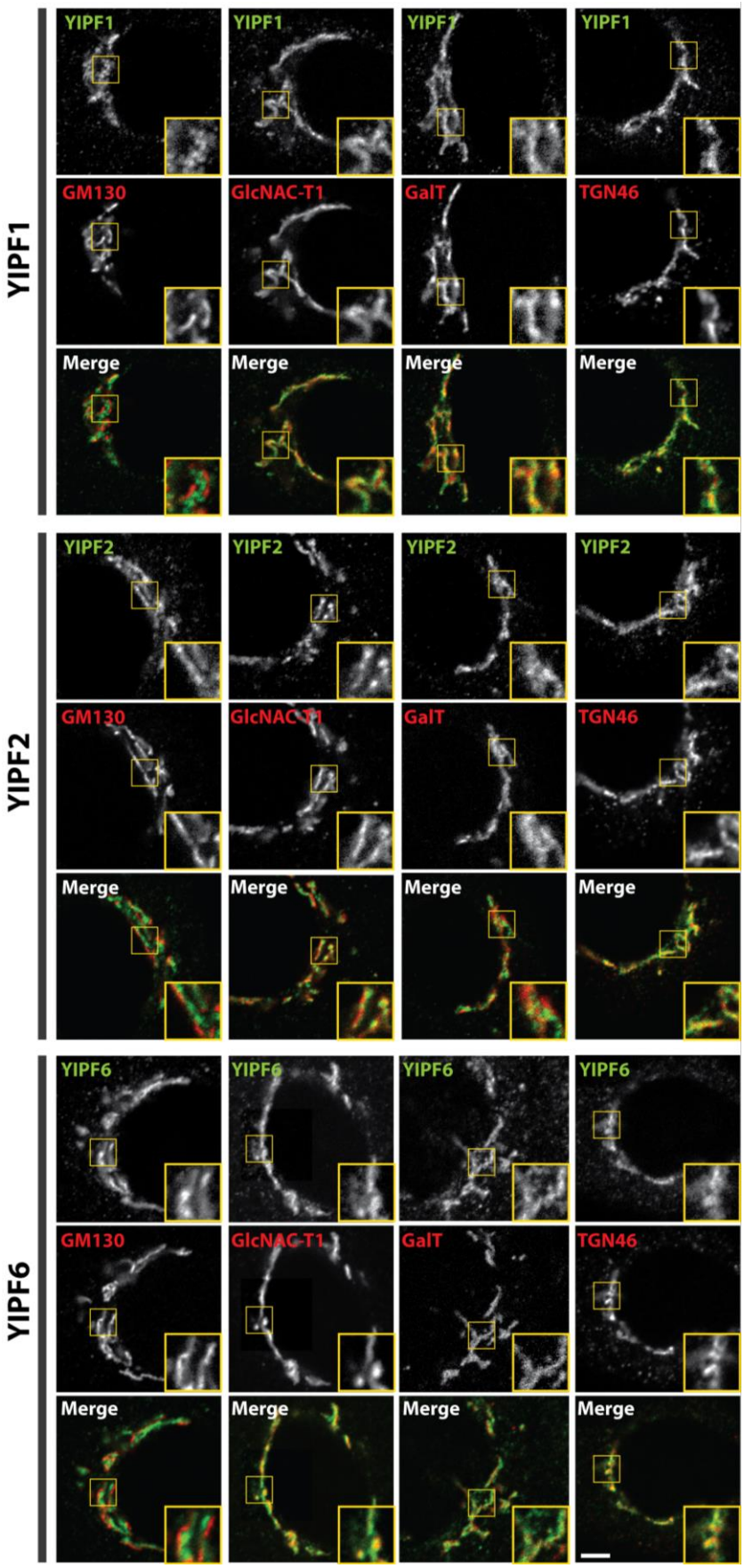
YIPF1
YIPF1
YIPF1
YIPF1
YIPF1
GM130
GlcNAC-T1
GalT
TGN46
Merge
Merge
Merge
Merge
YIPF2
YIPF2
YIPF2
YIPF2
YIPF2
GM130
GlcNAC-T1
GalT
TGN46
Merge
Merge
Merge
Merge
YIPF6
YIPF6
YIPF6
YIPF6
YIPF6
GM130
GlcNAC-T1
GalT
TGN46
Merge
Merge
Merge
Merge

Figure 12

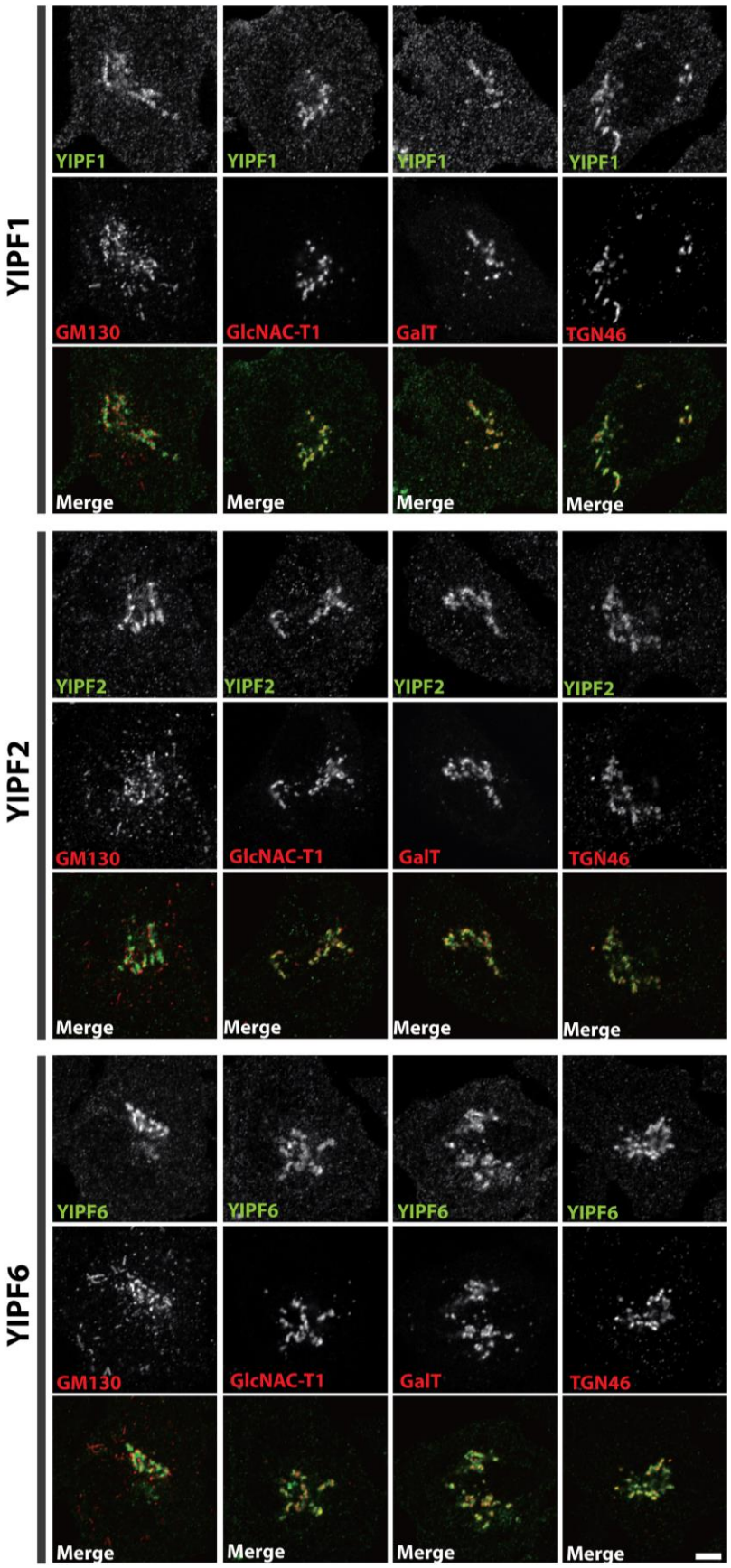
YIPF1
YIPF1
YIPF1
YIPF1
YIPF1
GM130
GlcNAC-T1
GalT
TGN46
Merge
Merge
Merge
Merge
YIPF2
YIPF2
YIPF2
YIPF2
YIPF2
GM130
GlcNAC-T1
GalT
TGN46
Merge
Merge
Merge
Merge
YIPF6
YIPF6
YIPF6
YIPF6
YIPF6
GM130
GlcNAC-T1
GalT
TGN46
Merge
Merge
Merge
Merge

Figure 13

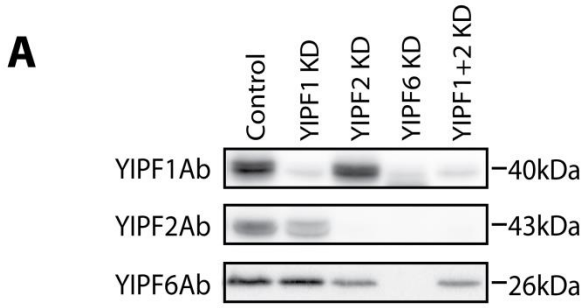
A
Control
YIPF1 KD
YIPF2 KD
YIPF6 KD
YIPF1+2 KD
YIPF1Ab
YIPF2Ab
YIPF6Ab
40kDa
43kDa
26kDa

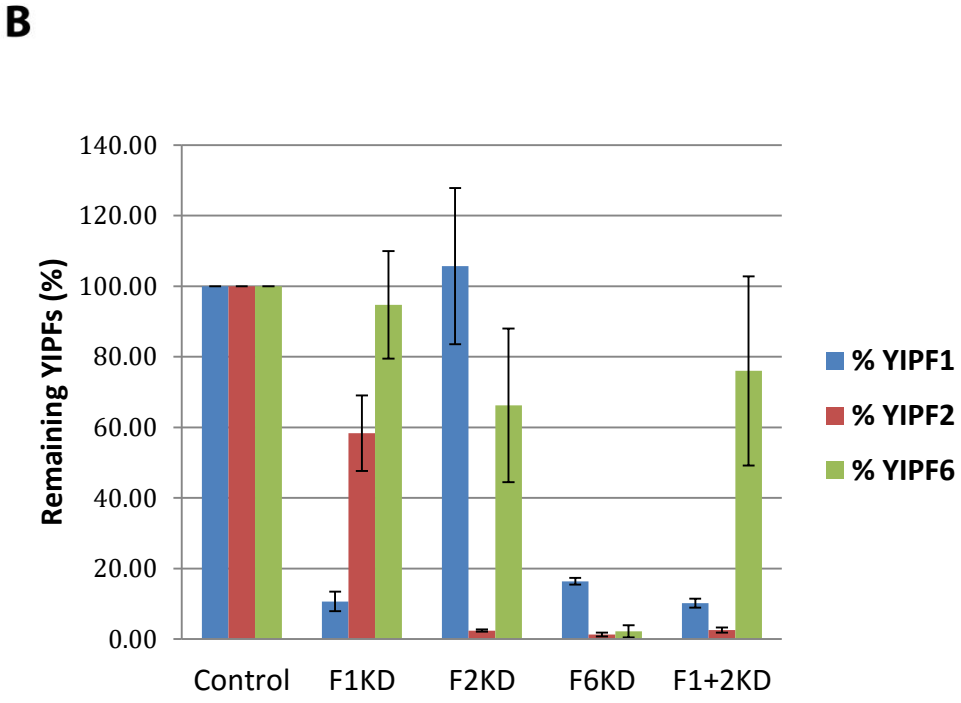
B
Remaining YIPFs (%)
140.00
120.00
100.00
80.00
60.00
40.00
20.00
0.00
Control
F1KD
F2KD
F6KD
F1+2KD
% YIPF1
% YIPF2
% YIPF6

Figure 14

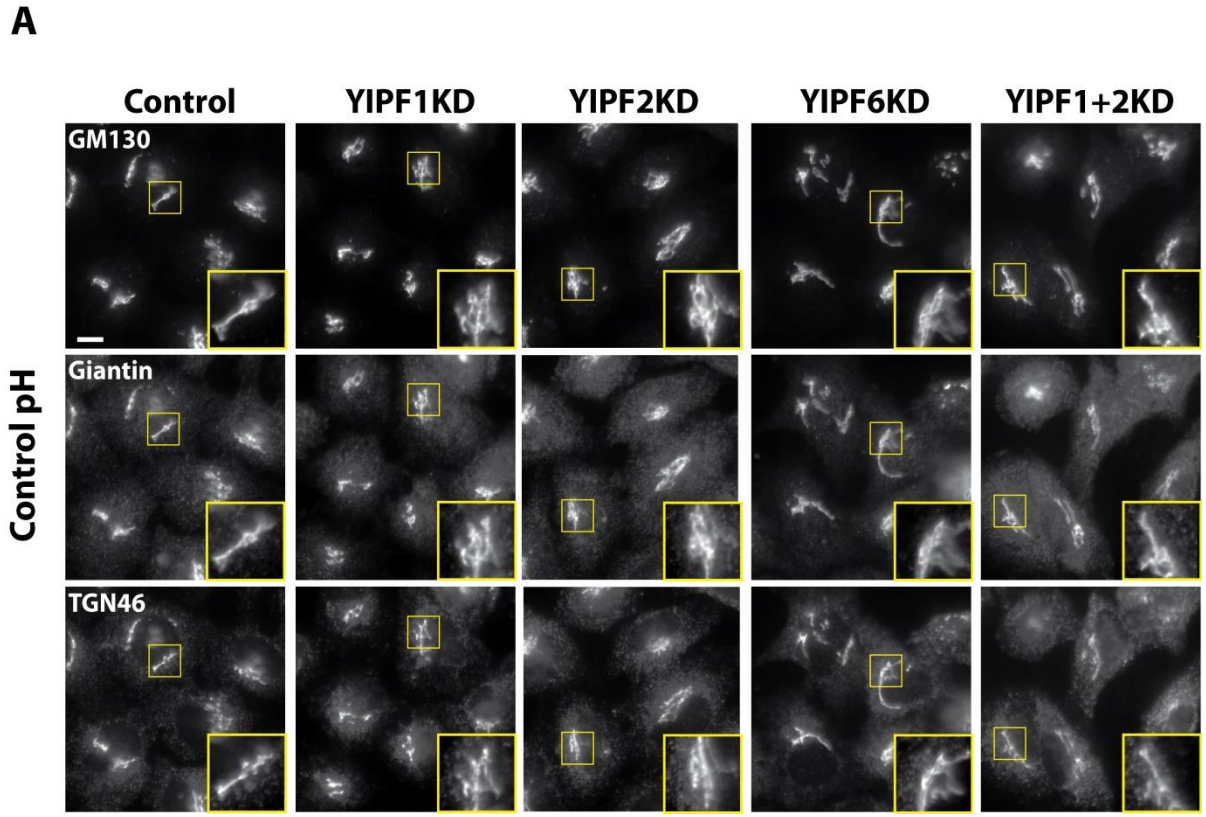
A
Control
YIPF1KD
YIPF2KD
YIPF6KD
YIPF1+2KD
GM130
Giantin
TGN46
Control pH

Figure 14

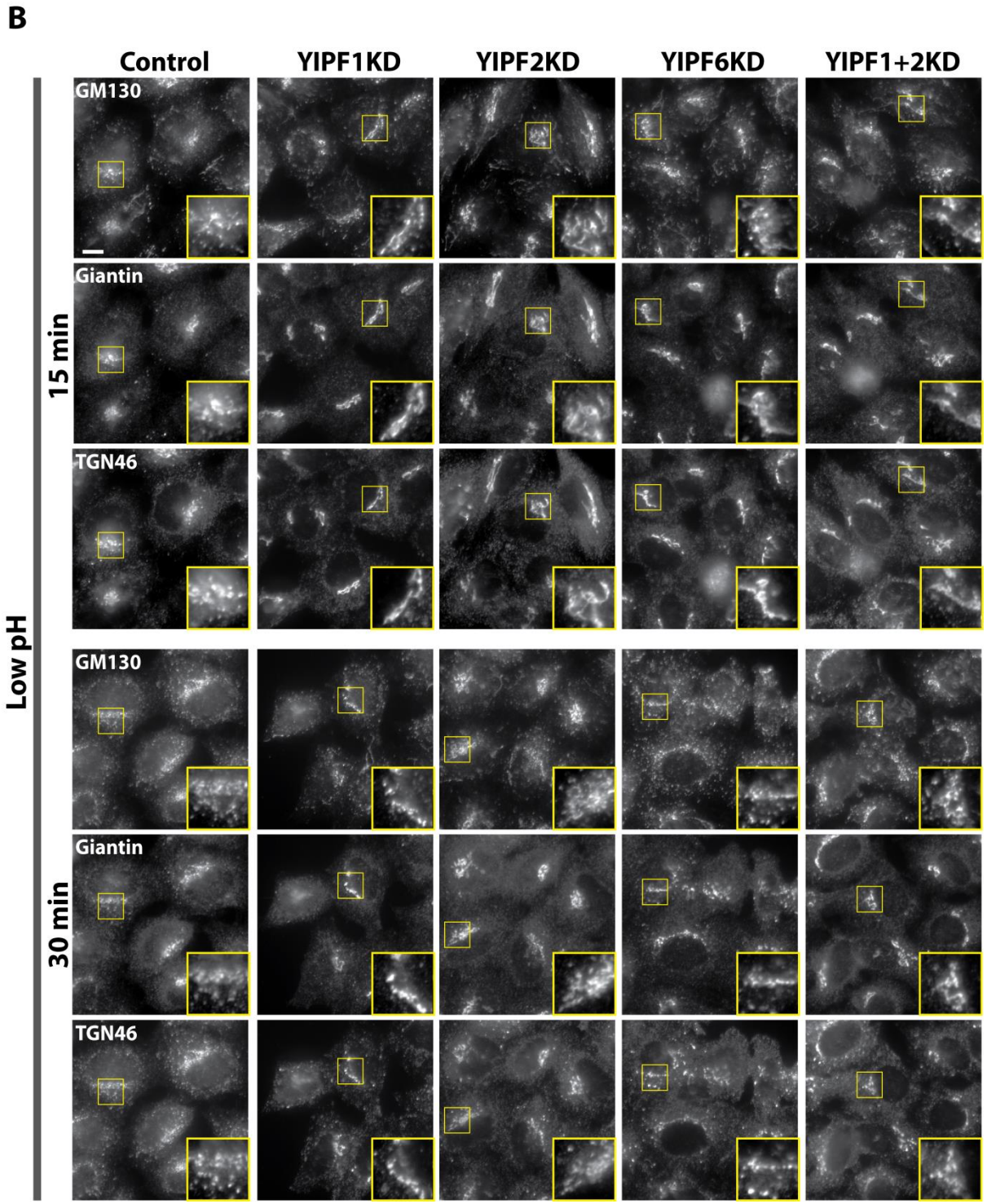
B
Control
YIPF1KD
YIPF2KD
YIPF6KD
YIPF1+2KD
GM130
Giantin
TGN46
GM130
Giantin
TGN46
15 min
30 min
Low pH

Figure 15

A

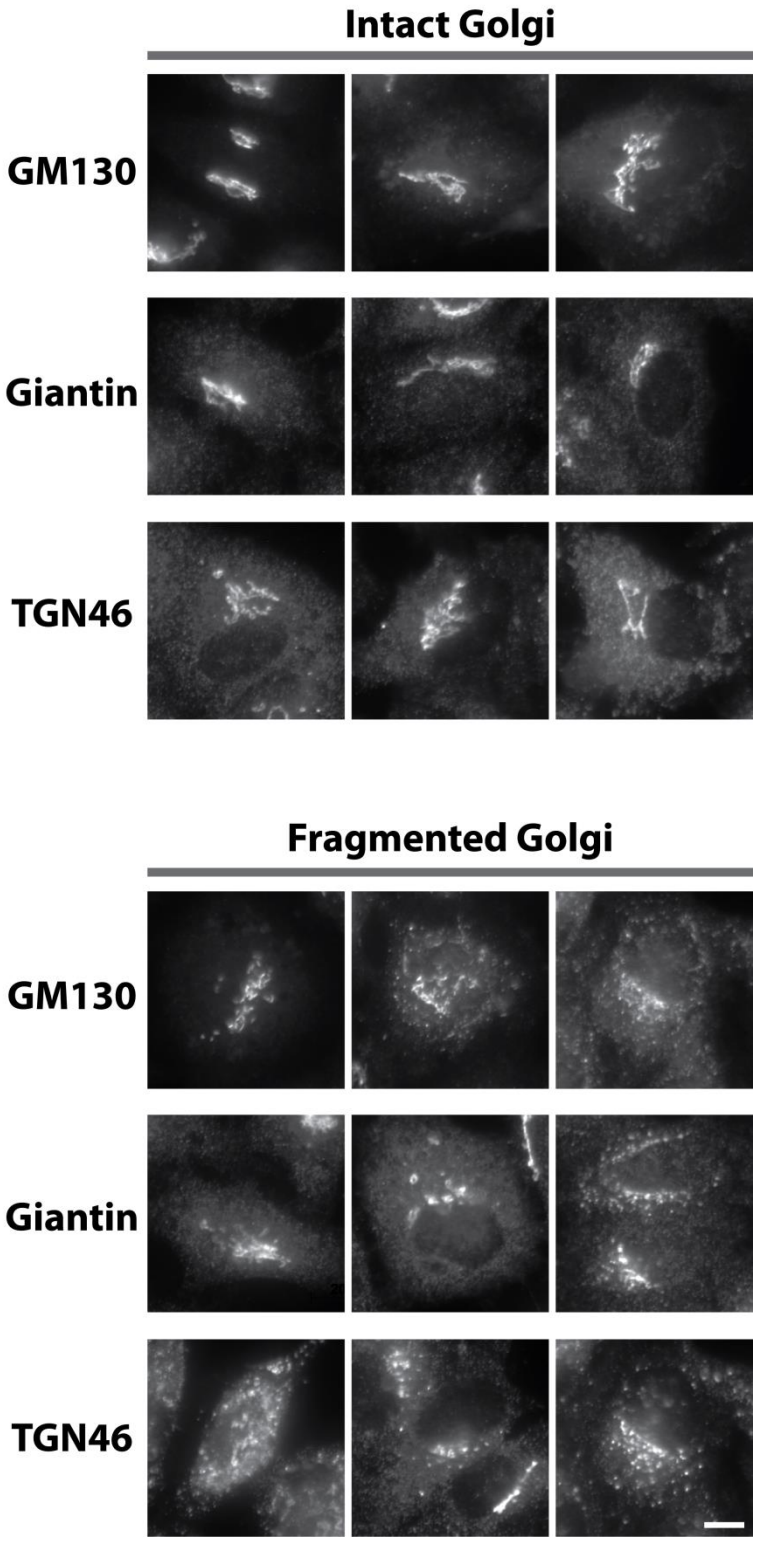
Intact Golgi
GM130
Giantin
TGN46
Fragmented Golgi
GM130
Giantin
TGN46

Figure 15

B

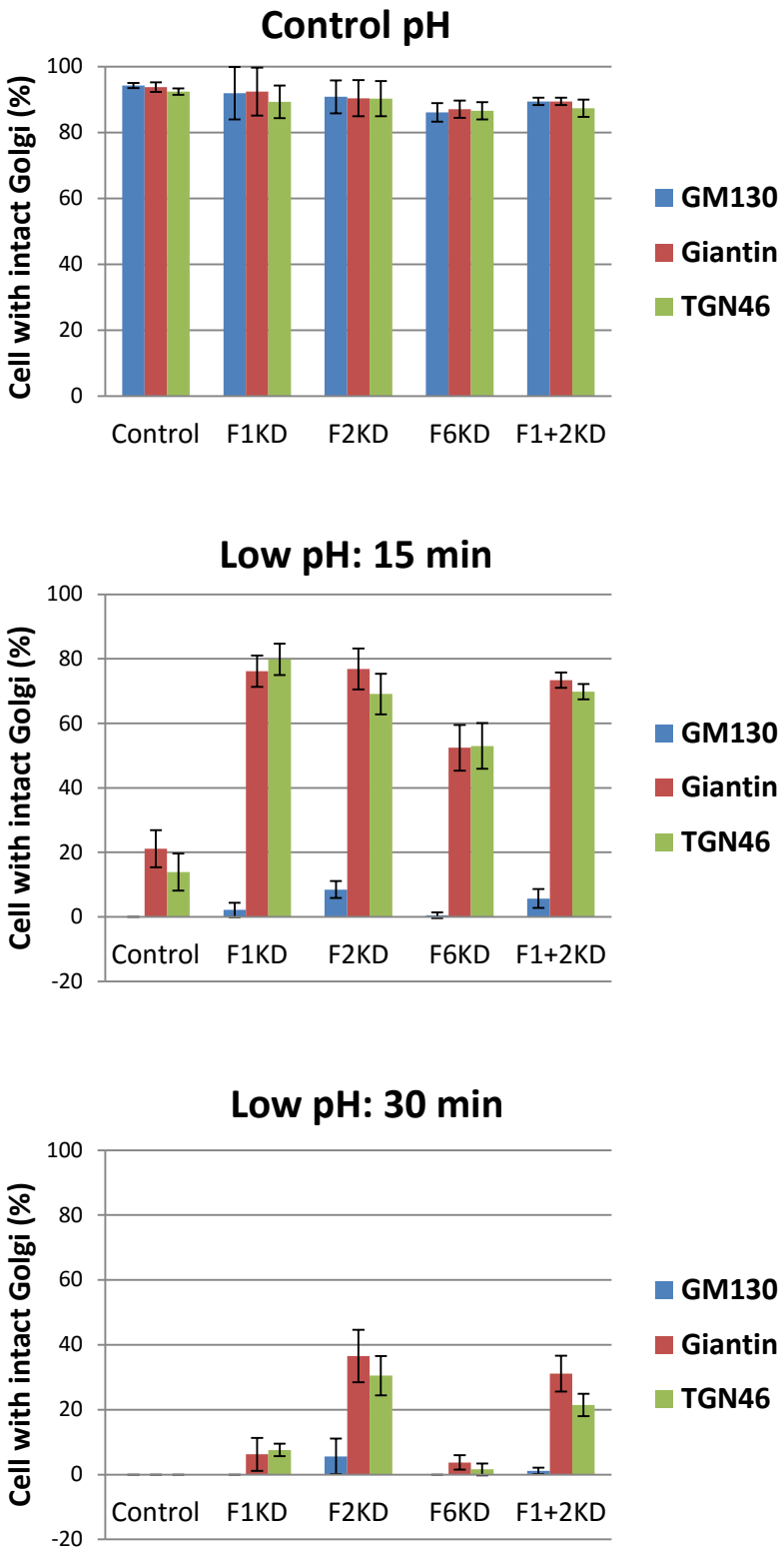
Control pH
Cell with intact Golgi (%)
100
80
60
40
20
0
Control
F1KD
F2KD
F6KD
F1+2KD
GM130
Giantin
TGN46
Low pH: 15 min
Cell with intact Golgi (%)
100
80
60
40
20
0
-20
Control
F1KD
F2KD
F6KD
F1+2KD
GM130
Giantin
TGN46
Low pH: 30 min
Cell with intact Golgi (%)
100
80
60
40
20
0
-20
Control
F1KD
F2KD
F6KD
F1+2KD
GM130
Giantin
TGN46

Figure 16

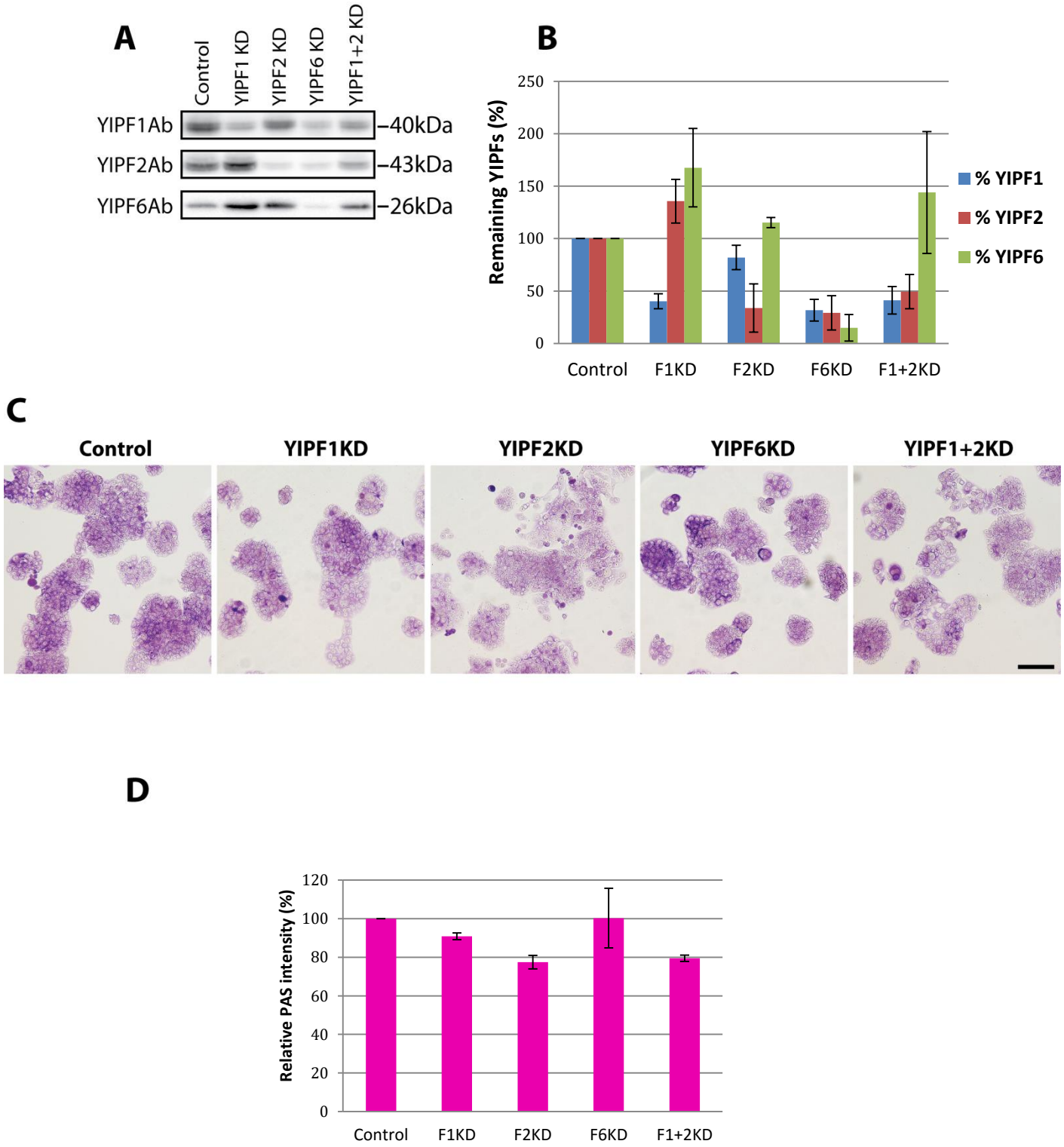
A
Control
YIPF1 KD
YIPF2 KD
YIPF6 KD
YIPF1+2 KD
YIPF1Ab
YIPF2Ab
YIPF6Ab
–40kDa
–43kDa
–26kDa
B
Remaining YIPFs (%)
250
200
150
100
50
0
Control
F1KD
F2KD
F6KD
F1+2KD
% YIPF1
% YIPF2
% YIPF6
C
Control
YIPF1KD
YIPF2KD
YIPF6KD
YIPF1+2KD
D
Relative PAS intensity (%)
120
100
80
60
40
20
0
Control
F1KD
F2KD
F6KD
F1+2KD